[American Journal of Science, Vol. 304, March, 2004, P. 250–284]

NUMERICAL ANALYSIS OF SEAWATER CIRCULATION IN CARBONATE PLATFORMS: II. THE DYNAMIC INTERACTION BETWEEN GEOTHERMAL AND BRINE REFLUX CIRCULATION

GARETH D. JONES*†, FIONA F. WHITAKER**, PETER L. SMART* and WARD E. SANFORD***

ABSTRACT. Density-driven seawater circulation may occur in carbonate platforms due to geothermal heating and / or reflux of water of elevated salinity. In geothermal circulation lateral contrasts in temperature between seawater and platform groundwaters warmed by the geothermal heat flux result in upward convective flow, with colder seawater drawn into the platform at depth. With reflux circulation, platform-top waters concentrated by evaporation flow downward, displacing less dense underlying groundwaters. We have used a variable density groundwater flow model to examine the pattern, magnitude and interaction of these two different circulation mechanisms, for mesosaline platform-top waters (50 ‰) and brines concentrated up to saturation with respect to gypsum (150 ‰) and halite (246 ‰). Geothermal circulation, most active around the platform margin, becomes restricted and eventually shut-off by reflux of brines from the platform interior towards the margin. The persistence of geothermal circulation is dependent on the rate of brine reflux, which is proportional to the concentration of platform-top brines and also critically dependent on the magnitude and distribution of permeability. Low permeability evaporites can severely restrict reflux whereas high permeability units in hydraulic continuity enhance brine transport. Reduction in permeability with depth and anisotropy of permeability (kv << kh) focuses flow laterally in the shallow subsurface (<1 km), resulting in a horizontally elongated brine plume. Aquifer porosity and dispersivity are relatively minor controls on reflux. Platform brines can entrain surficial seawater when brine generating conditions cease but the platform-top remains submerged, a variant of reflux we term "latent reflux". Brines concentrated up to gypsum saturation have relatively long residence times of at least 100 times the duration of the reflux event. They thus represent a long-term control on post-reflux groundwater circulation, and consequently on the rates and spatial patterns of shallow burial diagenesis, such as dolomitization.

INTRODUCTION

Groundwater circulation in carbonate rocks is important for understanding topics as diverse as management of groundwater resources (Oberdorfer and Buddemier, 1988), transport of contaminants (Muldoon and others, 1998) and hydrocarbon migration (Tator and Hatfield, 1975). Groundwater circulation is also an important control on carbonate diagenesis, which impacts subsequent flow via modifications to the porosity and permeability network. Of particular significance is the role of groundwater circulation in the formation of secondary replacement dolomites, which remains enigmatic despite its fundamental role in controlling spatial variations in hydrocarbon reservoir quality (Amthor and others, 1994; Saller and Henderson, 1998).

There has been increasing recognition over the past decade that early diagenesis of carbonates does not cease beneath the zone of meteoric water, and that active circulation of sea-water derived fluids can drive diagenesis within the shallow to intermediate burial zone (Whitaker and others, 1994). In part I we examined geothermal circulation (fig. 1A), which arises from variations in fluid density controlled by

*School of Geographical Sciences, University of Bristol, Bristol BS8 1SS, United Kingdom
**Department of Earth Sciences, University of Bristol, Bristol BS8 1RJ, United Kingdom
***United States Geological Survey, MS 430, Reston, Virginia 20192, USA
†Present address: ExxonMobil Upstream Research Company, P.O. Box 2189, Houston, Texas 77027, USA; email: gareth.d.jones@exxonmobil.com

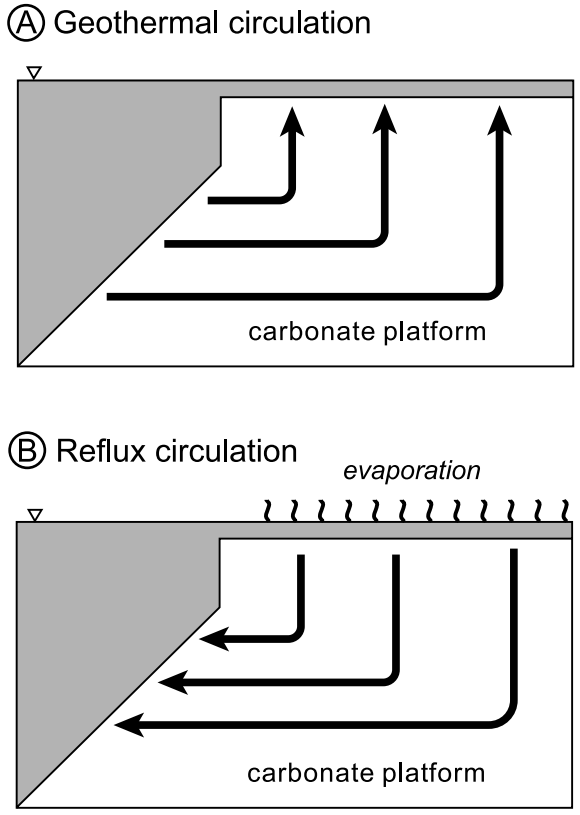

Fig. 1. Conceptual models of density-driven circulation in half a symmetrical isolated carbonate platform, (A) geothermal circulation, (B) reflux circulation.

differences in temperature between platform groundwaters and the surrounding ocean, in isolation from other potential drives for flow (Sanford and others, 1998). In this companion paper we consider the interaction between geothermal circulation and reflux, a flow system driven by differences in fluid density generated by spatial variations in the salinity. Evaporation of isolated or restricted bodies of seawater can result in the generation of brines, that subsequently flow downwards under the influence of gravity displacing less dense pore fluids (fig. 1B). Conceptual and analytical models suggest that refluxing brines will continue moving downwards until a depth at which their density equals that of the surrounding sea-water, and then flow laterally to discharge from the platform margins (Simms, 1984; Whitaker and Smart, 1993).

Reflux circulation was first proposed by Adams and Rhodes (1960) to explain replacement dolomitization of Permian reefs in West Texas, which show a close stratigraphic association with bedded evaporites. Reflux circulation has since been widely advocated to explain dolomitization in many carbonate platforms, particularly those proximal to hypersaline environments (see for example, Fisher and Rodda, 1969; Moore, and others, 1988; Shields and Brady, 1995; Pomar and Ward, 1999).

Adams and Rhodes (1960) developed the original model of reflux from associations in the rock record rather than observation of an active flow system. A number of more recent hydrological studies confirm that reflux operates in nature at a range of

scales. In the MacLeod evaporite basin, Australia, gypsum and halite saturated brines reflux through the underlying sedimentary units along the margins of an extensive (30 km wide) lagoon (Logan, 1987). At a much smaller scale, episodic reflux occurs on Cluett Key, Florida, from a hypersaline (<145 ‰) pond that is 100 meters in diameter (Juster and others, 1997). Even a minor increase in the salinity of seawater up to 42 permil is sufficient to drive regional-scale reflux circulation on the northwest Great Bahama Bank (Whitaker and Smart, 1990). Thus, the absence of evaporite facies in carbonate platforms does not preclude mesohaline brine reflux (Melim and Scholle, 2002). Brine driven flow systems are also known in a range of other geological settings, including around salt domes (Hanor, 1987; Evans and Nunn, 1989), beneath playa lakes (Lyons and others, 1995; Fan and others, 1997) and artificial brine disposal ponds (Simmons and Narayan, 1997; Uwiera, ms, 1998).

The driving force for reflux is the density gradient between platform-top brines and underlying platform groundwaters. However, the volume of brine refluxing will also depend on the areal extent of brine generation, which is determined by the interaction between platform morphology, sea level and climate (Burchette and Wright, 1992; Whitaker and Smart, 1993). Shallow flooding of rimmed shelves with characteristic broad flat tops, for example the Great Bahama Bank, can result in extensive areas of platform-top brine generation on the order of tens of kilometers. In contrast the very low depositional slopes (<1°) of homoclinal ramps, such as currently developed along the Trucial Coast in the Persian Gulf, limit brine generation to a relatively narrow zone, on the order of a few kilometers, adjacent to the shoreline.

When sea level drops below the platform-top on a rimmed shelf or rises to flood the platform top with normal seawater, brine generating conditions may be terminated. In contrast, on a homoclinal ramp although there is only a narrow zone of brine generation, this can be maintained by lateral migration in response to sea level changes (Burchette and Wright, 1992; Whitaker and Smart, 1993). The rate and distribution of reflux circulation will also be dependent on the magnitude and distribution of permeability (Whitaker and Smart, 1993). Finally, as with solute plumes in shallow aquifers, the degree of mixing (dispersion) along the flow path will also control the extent of the resultant reflux brine plume.

A number of theoretical studies have previously investigated fluid flow arising from salinity variations in a porous media, including those of Nield (1968), Sarkar and others (1995), Wooding and others (1997), and Sharp and others (2001). However, the application of dimensionless numbers, for example the Rayleigh number, to predict the expected flow dynamics is limited by a failure to incorporate the natural heterogeneity in rock properties (Schincario and others, 1997; Simmons and others, 2001). Furthermore, relatively few studies have focused on reflux circulation in carbonate platforms. The analytical investigations of Simms (1984) and Phillips (1991) and the laboratory experiments of Simms (1984) suggest that in addition to hypersaline brines, mesosaline brines with salinities only slightly greater than seawater can induce reflux. Numerical simulations of reflux beneath a 10 kilometer wide silled lagoon (Kaufman, 1994), demonstrate that the magnitude and lateral extent of the flow system are proportional to the brine concentration and the underlying sediment permeability. Kaufman's (1994) study provides some useful preliminary insights and demonstrates the potential utility of numerical simulations to systematically explore the nature and controls on reflux circulation. However, in common with previous studies, Kaufman considers reflux in isolation from other drives for flow. Evidence from modern hydrological systems (Whitaker and Smart, 1990; Juster and others, 1997; Wood and others, 2002) indicates that the interaction between reflux circulation and other flow systems may be important, and such complexities have been recognized in interpretations of paleo-reflux (Meyers and others, 1997; Mresah, 1998).

TABLE 1

Governing equations

Fluid mass	$\frac{\partial(\phi\rho)}{\partial t} = -\nabla\cdot(\phi\rho\mathbf{v})$	(1)
Fluid velocity	$\mathbf{v} = -\frac{\boldsymbol{k}}{\phi\mu}\cdot(\nabla p - \rho\mathbf{g})$	(2)
Thermal energy	$\frac{\partial\left[\phi\rho c_f + (1-\phi)\rho_s c_s\right]T}{\partial t} = -\nabla\cdot\lambda\nabla T + \nabla\left(\phi\rho c_f\,\mathbf{v}\right) + Q$	(3)
Thermal conductivity	$\lambda = \lambda_f\phi + \lambda_s(1-\phi)$	(4)
Solute mass	$\frac{\partial(\phi\rho)C}{\partial t} = -\nabla\cdot(\phi\rho\mathbf{v}C) + \nabla\cdot\left[\phi\rho(D_m + \boldsymbol{D})\cdot\nabla C\right]$	(5)
Dispersion coefficient	$D_{ii} = (1/v)\,(\alpha_L v_i^2 + \alpha_T v_j^2)$	(6.1)
	$D_{jj} = (1/v)\,(\alpha_T v_i^2 + \alpha_L v_j^2)$	(6.2)
	$D_{ij} = (1/v)\,)\,(\alpha_L - \alpha_T)\,(v_i v_j)\;\; i \neq j$	(6.3)
Fluid density	$\rho = 1025 + \left(-0.067417\cdot T - 0.0388\cdot T^2\right) + 0.7\cdot(C-36)$	(7)
Fluid viscosity	$\mu = 239.4\cdot10^{-7}\cdot10^{\frac{248.37}{T+133.15}}$	(8)

Here we consider the interaction between geothermal and reflux circulation for the case of platform top brines in a subtidal environment. Supratidal environments where there may be upward movement of groundwater by evaporative pumping or topographically-driven flow of meteoric groundwater to the coast (Hsu and Siegenthaler, 1969; Perkins and others, 1994; Wood and others, 2002) are beyond the scope of our study. Neither do we include the effect of compaction, which other modeling studies suggest drives flow at rates of 10^{-5} to 10^{-3} m/yr, several orders of magnitude less than those typical for geothermal convection (Whitaker and others, 2004). Specifically we address the following questions: (1) How does reflux interact with geothermal circulation? (2) How does this interaction evolve with time? (3) What is the fate of reflux brines between reflux events? (4) What is the effect and hierarchy of controlling parameters such as platform-top brine concentration, sea level, porosity, permeability, permeability anisotropy, dispersivity and platform geometry?

NUMERICAL MODEL

To analyze geothermal and reflux circulation we solve the partial-differential equations representing transient fluid flow and heat and solute transport in a porous medium (table 1, eqs 1, 2, 3 and 4). We solve the governing equations presented in table 1 numerically, using the variable density groundwater flow model SUTRA (Voss, 1984; http://water.usgs.gov/nrp/gwsoftware/sutra/sutra.html), modified to solve the interdependent processes of fluid flow with heat and solute transport. The numerical

TABLE 2
Symbol notation

Symbol	Description	Unit	Values
C	Salinity	$^{o}/_{oo}$	computed
c_f	Specific heat capacity of fluid	J/kg/°C	4950
c_s	Heat capacity of solid grains	J/kg/°C	950
$\mathbf{D}$	Dispersion tensor	m^2/s	computed
D_m	Coefficient of diffusion	m^2/s	10^{-9}
D_x	Horizontal dispersion	m^2/s	computed
D_z	Vertical dispersion	m^2/s	computed
$\mathbf{g}$	Gravitational acceleration	m^2/s	9.8
$\mathbf{k}$	Permeability	m^2	Computed
Q	Heat flux	W/m^2	0.06
p	Fluid pressure	Pa	computed
T	Temperature	°C	computed
t	Time	s	computed
$\mathbf{v}$	Velocity	m/s	computed
$\mathbf{v_x}$	Horizontal velocity	m/s	computed
$\mathbf{v_z}$	Vertical velocity	m/s	computed
α_L	Horizontal dispersivity	m	10^2
α_T	Vertical dispersivity	m	10
λ	Effective thermal conductivity	J/s/m/°C	computed
λ_f	Thermal conductivity of fluid	J/s/m/°C	0.6
λ_s	Thermal conductivity of solid grains	J/s/m/°C	3.3
ϕ	Porosity	dimensionless	computed
ρ	Density of fluid	Kg/m^3	computed
ρ_s	Density of solid grains	Kg/m^3	2650
μ	Fluid viscosity	Kg/m/s	computed

algorithm used to solve these equations is exactly equivalent to that of SUTRA, except that both the heat and solute transport equations are solved (in order to update the fluid density) after the flow equation within each time-step iteration. The bulk thermal conductivity is a volumetric average of the water and the rock (table 1, eq 5). The dispersion coefficient is computed from the horizontal and vertical dispersion coefficients (Voss, 1984; table 1, eqs 6.1 and 6.2). Fluid density is specified to be a non-linear function of temperature (Sanford and others, 1998) and a linear function of salinity (Voss, 1984; table 1, eq 7). Fluid viscosity is specified as a non-linear function of temperature (Sanford and others, 1998), and for the range investigated we assume the effect of salinity on viscosity is negligible (Ophori, 1998; table 1, eq 8). These equations-of-state for fluid density and viscosity are less sophisticated than other algorithms available (see review by Adams and Bachu, 2000). We tested the validity of our equations-of-state for fluid density and viscosity by simulating reflux with Basin2 (Bethke and others, 1999; release 4.1) that employs the relationships of Phillips and others (1981). We report that, at the scale of interest, the distributions of fluid flow, temperature and salinity were similar and did not change our interpretation of results derived using our modified version of SUTRA (Jones, 2003). Symbol notation and values used in this study are defined in table 2.

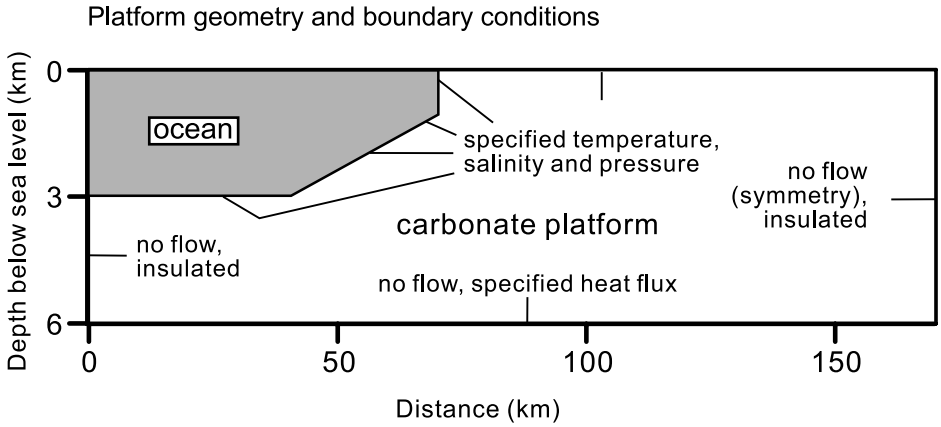

Fig. 2. Platform geometry and boundary conditions for half a symmetrical isolated rimmed shelf carbonate platform.

In order to reduce computational time we simulate a half-platform with a symmetry boundary at the right side (fig. 2). The majority of our sensitivity analyses are conducted for this rimmed shelf platform geometry with an ocean depth of 3 kilometers and a half-platform width of 100 kilometers. We also simulate geothermal and reflux circulation in homoclinal and distally steepened ramp type platforms, which have different geometries (and platform-top brine configurations) that are described later. The flow domain is discretized with a uniform horizontal node spacing of 5 kilometers and a vertical node spacing of 50, 100 and 200 meters from the platform top to depths of 3, 4 and 6 kilometers respectively. Results derived from regional scale simulations of density driven flow tend to be less dependent on grid dimensions than reported at a more local scale (Diersch and Kolditz, 2002; Craig Simmons, personal communication). We tested the effect of two additional grids, both finer scale than the one described above, and report that for the reflux of gypsum saturated brines our results were independent of the grid dimensions tested (Jones, ms, 2000). Side boundaries are specified to be no-flow and insulated. A geothermal heat flux of 60 mW/m^2 is assigned to the basal boundary (Griffen and others, 1977). We did not test the effect of substituting a constant temperature basal boundary for that of a specified heat flux. Ocean and platform-top boundary temperatures are specified using temperatures from the Tongue of the Ocean adjacent to the Great Bahama Bank (Busby and Dick, 1964). The basin and slope portion of the ocean boundary is specified with a uniform salinity of 36 permil. The salinity of platform-top waters is commonly observed to increase gradually from open water salinities of 36 permil at the margin towards maximum values in the platform center where restriction is greatest (Scruton, 1953; Traverse and Ginsburg, 1966; Purser, 1973). Thus to represent platform-top brine generation, salinity is specified to increase linearly from seawater (36 ‰) up to a maximum at the platform center (the right side symmetry boundary). The areal extent of platform-top brines can vary by orders of magnitude from local ponds 0.1 kilometer in width (Juster and others, 1997) to large lagoons 150 kilometers across (Fisher and Rodda, 1969). For rimmed shelves we chose 75 kilometers as the extent of platform-top brines, based on the distribution of elevated salinities observed on the present-day Great Bahama Bank (Traverse and Ginsburg, 1966), which is similar to that interpreted for the Upper Jurassic Smackover platform (Moore and others, 1988). We examine the effect of three different types of platform-top

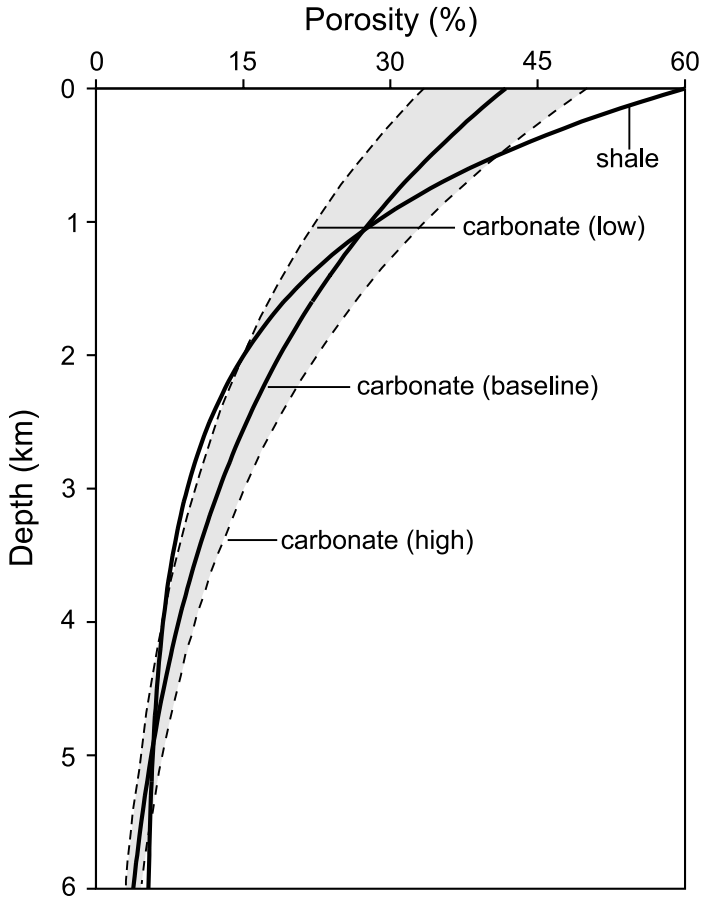

Fig. 3. Porosity versus depth relationships for carbonates (Schmoker and Halley, 1982) and basinal shales (Harrison and Summa, 1991). High and low curves are used in porosity sensitivity analysis (see text).

brines, defined by their maximum concentration as: mesosaline (salinity <50 ‰), gypsum saturation (salinity <150 ‰) and halite saturation (salinity <246 ‰). Ocean boundary fluid pressures are specified to be hydrostatic. The water depth across the platform-top is specified as 5 meters, allowing exchange of seawater between the shallow bank-top sea and adjacent ocean.

Carbonate rocks are often fractured and/or karstifed resulting in the generation of secondary porosity and permeability at a range of scales (Rovey and Cherkauer, 1995; Whitaker and Smart, 1997). However the dimensions of our grid elements are assumed to be greater than the representative elementary volume (REV) for the system investigated, and thus we use an equivalent porous medium (EPM) approximation for secondary porosity and permeability. As we have previously shown, the distribution of porosity (and hence permeability) with depth has a major impact on the magnitude and extent of subsurface circulation in model carbonate platforms (Sanford and others, 1998). Therefore, unlike for our previous study of geothermal circulation, we adopt a more realistic model of varying porosity with depth as standard for all simulations. We use the best fit relationship for carbonate rocks developed by Schmoker and Halley (1982) for Cenozoic and Mesozoic carbonates of South Florida (fig. 3).

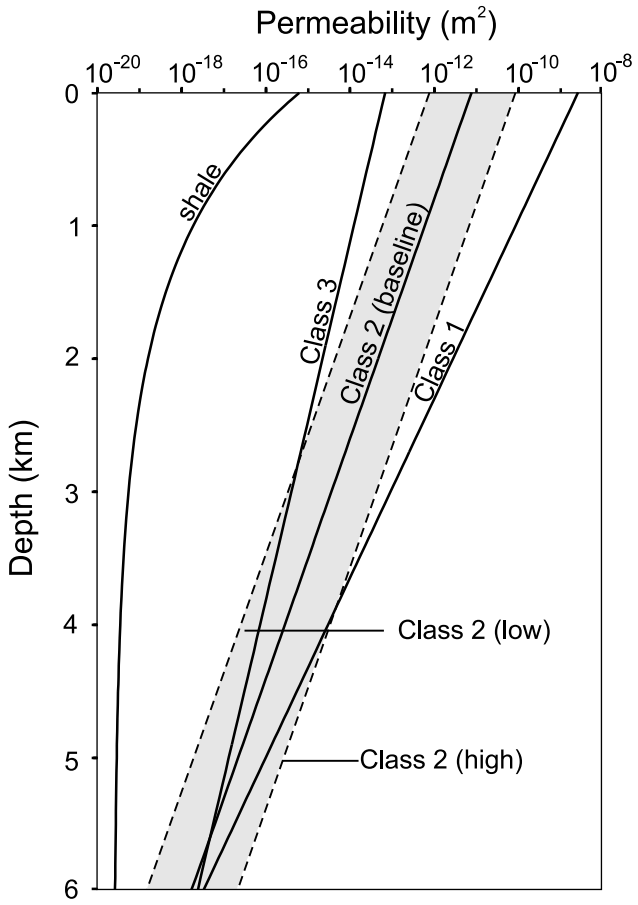

Fig. 4. Permeability calculated from porosity as a function of depth for carbonate grainstones (Class 1), packstones (Class 2) and mudstones (Class 3) after Lucia (1995) and shales (Harrison and Summa, 1991). Class 2 curve is our carbonate permeability baseline, high and low curves are used in permeability sensitivity analysis (see text).

Permeability is calculated as a function of porosity using the empirical relationships of Lucia (1995) for carbonates (fig. 4). For our baseline simulation we use the Class 2 porosity-permeability relationship representative of packstone carbonate sediments (Lucia, 1995). Specifying the Class 1 (grainstone) porosity-permeability relationship for the entire platform is not possible because of numerical instability and conduction is therefore the dominant mode of heat transport in our simulations (see also Sanford and others, 1998). We note that the porosity-permeability relationship selected is often the principal cause of uncertainty in any investigation of regional scale groundwater flow (Jones and others, 1998) and address this uncertainty in our sensitivity analysis. Permeability anisotropy (the ratio of horizontal to vertical permeability) is specified as 1000 based on results of flow simulations designed to quantify regional-scale permeability anisotropy in sequences of carbonate rocks that exhibit laterally extensive horizons with secondary dissolutional porosity, cements or evaporite precipitates (Jones, ms, 2000). Diffusion coefficients for the common aqueous species in seawater are reasonably well constrained and we use a value of 10^{-9} m^2s^{-1} (Robinson and Stokes, 1965). In contrast, dispersivity is harder to estimate as it is strongly scale dependent (Gelhar,

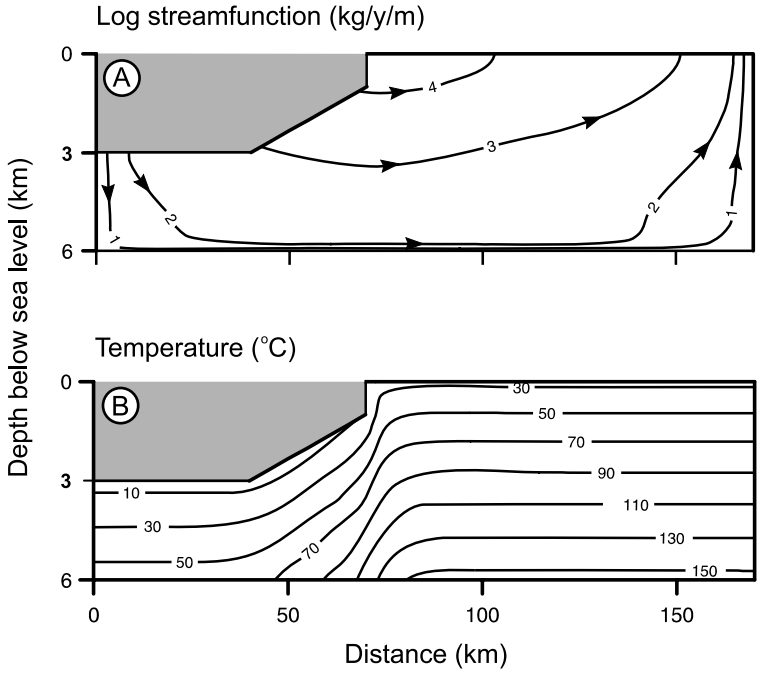

Fig. 5. Steady-state geothermal circulation used as initial conditions for simulations of reflux circulation. Initial platform salinity is 36 ‰.

1986). Based on the horizontal dimension of our mesh elements and the scaling relationship of Gelhar (1986) we specify a horizontal dispersivity of 100 meters. There is paucity of data in the literature on the anisotropy of dispersivity (the ratio of horizontal to vertical dispersivity), but we use a dispersivity anisotropy of 10 (Klotz and others, 1980).

We contour the mass-based streamfunction (Evans and Raffensperger, 1992) to define streamlines and to display the magnitude and distribution of fluid flux. The streamfunction is the cumulative horizontal fluid flux from z=1 to n, when n is the maximum elevation of the top model node, and it is calculated for each of the model columns from x=1 to m, when m is the number of nodes in the horizontal direction. In order to display the full range of circulation within the platform we employ logarithmic streamfunctions. These define stream tubes over which cumulative horizontal fluid flux increases by one order of magnitude. For simplicity we do not include the sign on the contoured stream function plots. At the interface between circulation systems which derive from the ocean (positive flux), and those which derive from the platform (negative flux) there is a steep gradient in streamfunction, the centerline of which defines the hydrologic boundary between the systems (dashed in figures). It is important to recognize that across this interval fluid flux varies little from that in adjacent cells, as indicated by convergence and tight packing of stream tubes.

Unless otherwise stated all of our simulations commence with initial fluid pressures and groundwater temperatures calculated for a conductive, steady-state field in a platform filled with unmodified seawater (salinity of 36 ‰). Under these initial conditions geothermal circulation draws seawater into the platform through the basin and slope to discharge through the platform-top (fig. 5A). With geothermal circulation, the greatest fluid flux ($>10^4$ kg/y/m) is focused at the platform margin and

isotherms in the corresponding temperature distribution (fig. 5B) parallel the ocean bathymetry indicating that conduction is the dominant mode of heat transport (Sanford and others, 1998).

In contrast to geothermal circulation, which can be treated as a steady-state problem (Sanford and others, 1998), reflux circulation is a time dependent problem that requires a transient solution. We examine the pattern and magnitude of evolving geothermal and reflux circulation for durations of up to 10 My. The controlling parameters we examine in the sensitivity analysis described below include boundary conditions on the platform top, a range of rock properties and platform geometry (table 3).

SENSITIVITY ANALYSIS

Boundary Conditions

Magnitude of platform-top salinity.—For mesosaline brines, salinities range from 50 permil at the platform center to 36 permil, 25 kilometers from the platform margin (represented schematically by the wedge above the platform in fig. 6.) The evolving pattern of fluid flux and salinity is depicted at times of 0.1, 0.3, 0.7 and 1 My after reflux commences (fig. 6). At relatively early times (<0.1 My) any reflux circulation that develops is below the minimum vertical scale of mesh resolution (50 m). After 0.1 My reflux circulation extends over a limited (<20 km wide) zone in the platform interior and penetrates to a depth of up to 200 meters before being forced to discharge through the platform-top by ascending geothermally-driven flow (fig. 6A). In all our streamfunction plots the dashed line is the boundary between flow driven by geothermal circulation and that driven by reflux (for example, fig. 6). At 0.1 My the total fluid flux driven by reflux (on the order of 10^2 kg/y/m) is two orders of magnitude less than that for geothermal circulation, which thus accounts for the majority of the fluid flux in the platform. For both geothermal and reflux circulation the fluid flux decreases dramatically with depth due to the specified reduction in permeability (fig. 6). The reflux brine plume is elongate, reflecting the anisotropy in permeability and dispersivity, and thickens towards the platform interior where vertical contrasts in fluid density are greatest (fig. 6B). Over time reflux circulation extends towards the platform margin and to increasing depth, progressively reversing the density gradient and reducing the extent of geothermal circulation from the platform interior (fig. 6C, E and G). By 1 My the brine plume extends over a zone up to 50 kilometers wide and penetrates to a depth of up to 2 kilometers, and geothermal circulation is limited to within 40 kilometers of the margin (fig. 6H). The total reflux-driven fluid flux has also increased to be comparable in magnitude with that of the geothermal circulation (10^4 kg/y/m), but the latter has not declined compared to initial conditions.

Comparison of simulations with mesosaline brines to those with platform-top brines concentrated up to gypsum saturation (fig. 7) and halite saturation (fig. 8) demonstrates the critical role of the fluid density gradient on the pattern and magnitude of reflux circulation, and the longevity of geothermal circulation. An increase in platform-top salinity results in increased brine recharge due to the enhanced density difference between surface and subsurface waters. Thus with more concentrated platform-top brines (up to 150 ‰ in fig. 7 and up to 246 ‰ in fig. 8) regional-scale reflux circulation is established within 1 ky, compared to 100 ky for mesohaline brines (up to 50 ‰ in fig. 6). Note that initially (1 to 10 ky, figs. 7 and 8B and 8D) that most of the fluids driven by reflux are of seawater salinity as there has been insufficient time for their replacement by refluxing brines. Total fluid fluxes are comparable to those in the geothermal circulation, although the latter is already becoming restricted to the platform margin. Initially the brine-driven reflux circulation discharges at the platform top in areas occupied by brines of lower salinity than

TABLE 3

Controlling parameters, baseline values and parameter range/relationship tested

Parameter	Baseline	Range / Relationship	Figure(s)
Boundary Conditions			
Platform-top salinity	36–250 $^{o}/_{oo}$	Uniform 36 $^{o}/_{oo}$	5
		36–51 $^{o}/_{oo}$	6
		36-150 $^{o}/_{oo}$	7
		36–250 $^{o}/_{oo}$ (Isolated platform-top sub-basin)	8,10
	Continuous platform-top brine generation	One 0.1 My reflux event with platform-top brines of 36-150 $^{o}/_{oo}$ followed by a 10 My period of uniform 36 $^{o}/_{oo}$	11
		Series of alternating 0.1 My periods of on / off platform-top brines concentrated up to gypsum saturation (36-150 $^{o}/_{oo}$)	12
Rock Properties			
Porosity	Halley and Schmoker (1982)	+20 % of baseline curve	13
		-20 % of baseline curve	13
Permeability	Lucia (1995), Class 2 - (packstones)	Baseline curve x 10	14
		Baseline curve /10	14
		Lucia (1995), Class 1	N/A
Permeability anisotropy (k_x:k_z)	10^3	10^2	15
		10^4	15
Lateral permeability	No lateral variation	Aggrading platform	16
		Prograding platform	16
		Evaporite layer at depth of 300 – 1300 m	17
		Evaporite layer from surface – 1 km depth	17
Dispersivity	α_L = 100 m, α_T = 10 m	$\alpha_L = 10^2$ m, $\alpha_T = 10^2$ m	18
		$\alpha_L = 10^2$ m, α_T = 1 m	18
		$\alpha_L = 10^3$ m, α_T = 100 m	18
Platform Type			
	Rimmed shelf	Distally steepened ramp	19
		Homoclinal ramp	19

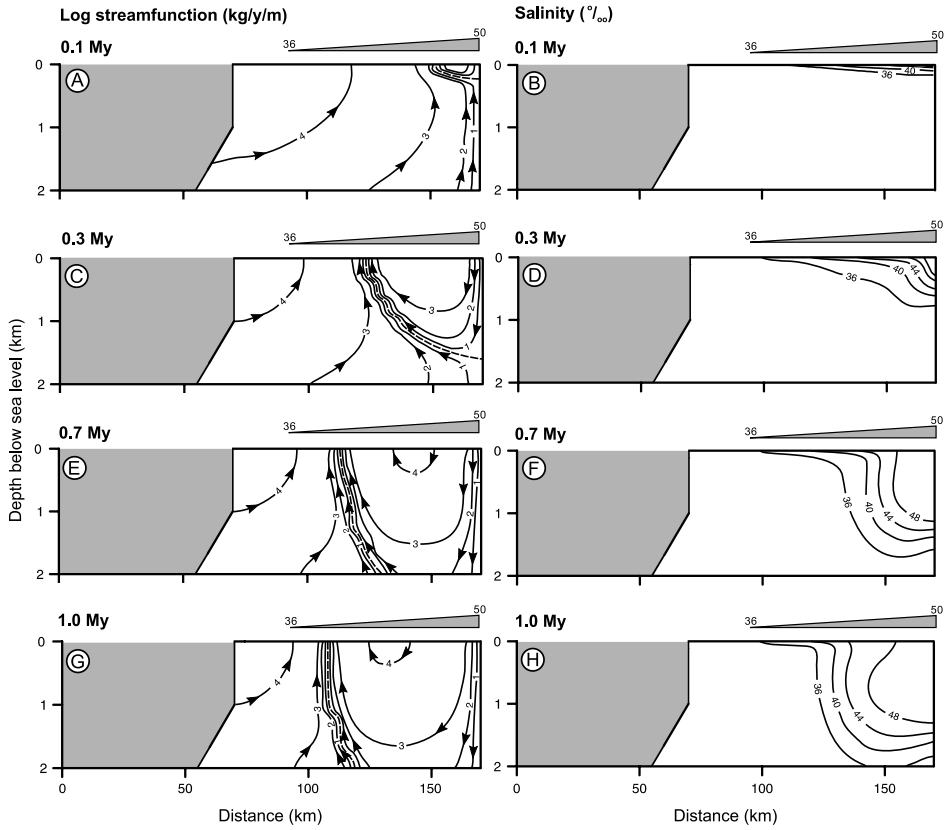

Fig. 6. Temporal evolution of geothermal and reflux circulation with mesohaline platform-top brines. Note only upper 2 km of platform displayed.

those recharged (fig. 7A and 7C, fig. 8A and 8C), but with time the circulation extends to discharge in the marginal platform top zone occupied by waters of normal sea-water salinity (figs. 7E and fig. 8C). At this time geothermal circulation continues in the platform margin, but this circulation cell is progressively eliminated as the brine-driven reflux circulation discharges initially at the top (fig. 8E) and then over the whole of the ocean platform margin (figs. 7G and 8G), a stage not reached in the mesohaline brine simulations (fig. 6G). The progressive lateral extension of the reflux circulation cell occurs about 10 times faster for the very dense halite saturated brines than for brines of maximum gyspum saturation (compare figs. 7E and 8C), whereas for the mesohaline brines the difference is about 100 times (compare figs. 7E and 8C). There is a progressive strengthening of the reflux circulation through time, most clearly seen in the increase of fluid flux for the halite saturated brine (fig. 8A to E), until fluid flux stabilizes once brines discharge laterally from the margin (fig. 8E, G). For the initial stages of reflux circulation (that is discharge at the platform top), the magnitude of the fluxes for the three brine densities are comparable (compare fig. 6A, 6C, 6E, 6G with fig. 7A, 7C, 7E, and fig. 8A, 8C). However, for a given lateral extent of the reflux circulation cell, the deeper circulation that occurs for the low salinity simulations actually gives a more extensive zone of high flux (log streamfunction >4 kg/y/m) than for brines of higher salinity. There is thus a greater volume of recharged brine in the platform for the mesosaline simulations than for those with higher salinity brines at a

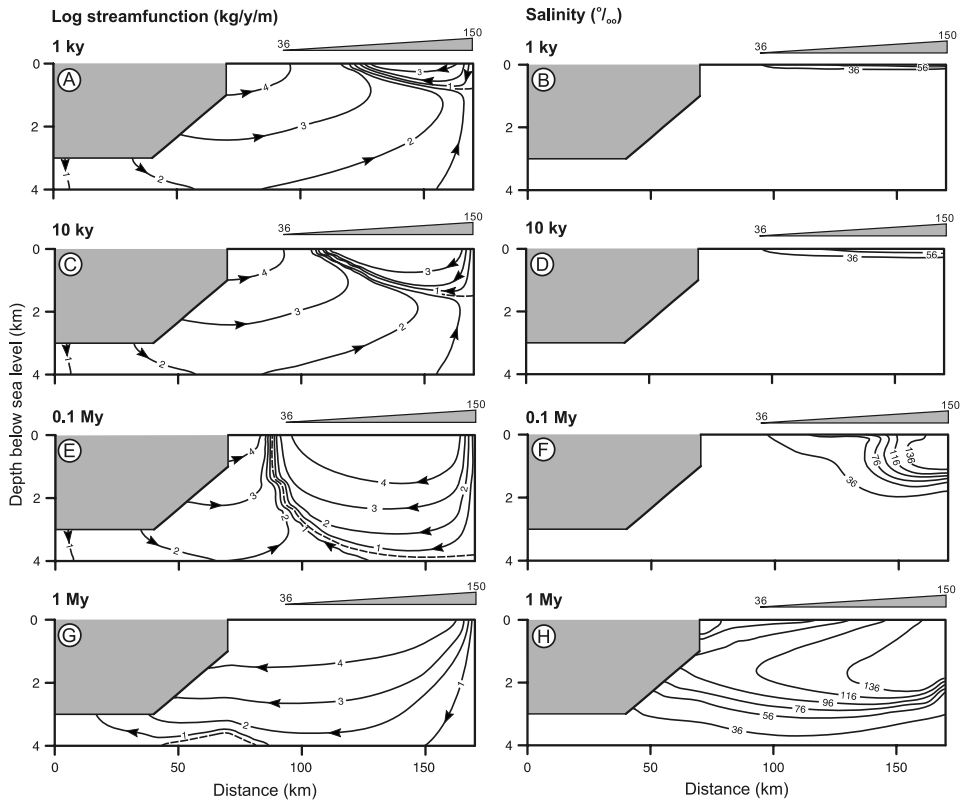

Fig. 7. Temporal evolution of geothermal and reflux circulation with platform-top brines concentrated up to gypsum saturation. Note upper 4 km of platform displayed.

comparable extent of the reflux circulation cell (compare figs. 6G and 6H, 7C and 7D, and 8A and 8B).

Once the reflux circulation extends to the platform margin, there is a substantial increase in fluid flux, which is strongly dependent on brine salinity (compare figs. 7G and 8E). At subsequent times the total fluid flux does not increase further. However, as would be expected, higher brine salinities result in more concentrated plumes that penetrate deeper and extend further towards the platform margin after the same interval of time (figs. 6, 7 and 8) because of the higher density gradients which cause the reflux circulation to develop more rapidly at higher salinities.

Our simulations suggest that reflux of platform-top brines has only a minor effect on groundwater temperatures. After 0.1 My of reflux circulation with brines concentrated up to halite saturation temperatures in the platform interior are reduced by less than 7 °C due to advective cooling (fig. 9). This effect is most significant at intermediate (c2 km) depths where the fluid flux is high (fig. 9B). This small change is due to the relatively low permeabilities used for carbonates in our simulations, and thus high rate of heat conduction compared to the rate of advective removal of heat by groundwater circulation (Sanford and others, 1998). The temperature change will cause a decrease of viscosity, and thus enhanced groundwater flow, but this effect will have only a minor effect on fluid flux. With mesosaline brines the platform temperatures show a similar pattern to that with hypersaline brines but the magnitude of the decrease is less than 1 °C (results not shown). The effect of reflux on temperatures was minor for the other

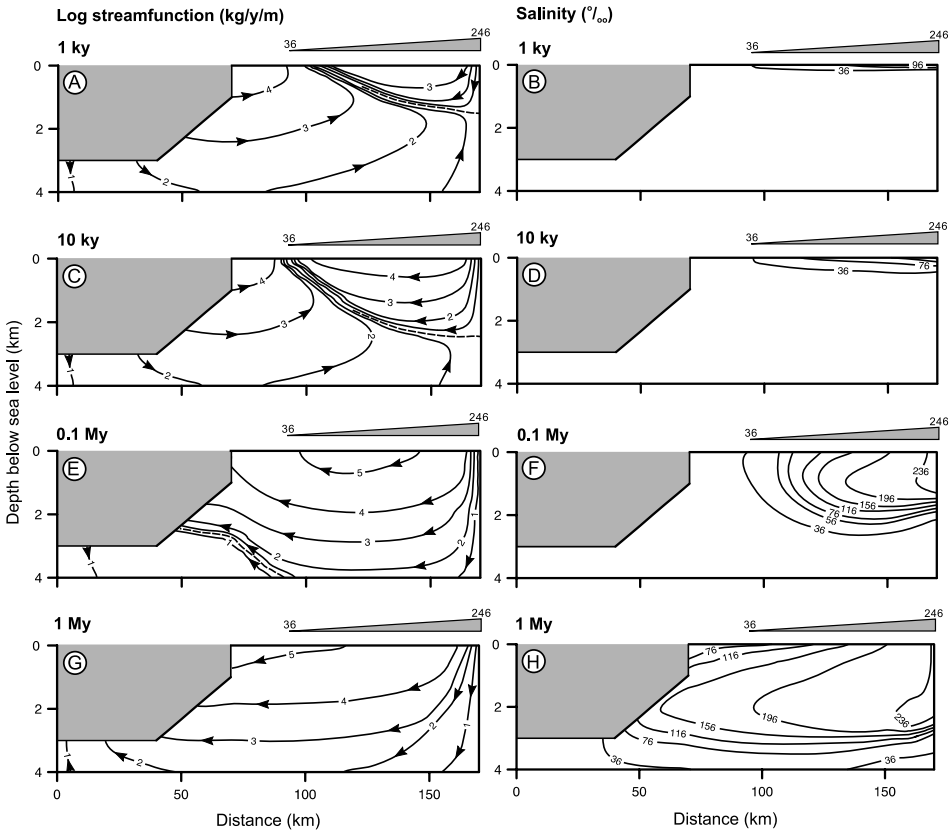

Fig. 8. Temporal evolution of geothermal and reflux circulation with platform-top brines concentrated up to halite saturation.

parameters tested in our sensitivity analysis (table 3) and in presenting our results below we therefore focus on the distribution of fluid flux and salinity.

Distribution of platform-top salinity.—In the above simulations we assume that restriction results in a gradual increase in salinity across the platform-top. In contrast some ancient platforms, for example the Upper Devonian Nisku platform (Switzer and others, 1994) exhibit isolated, but relatively extensive platform-top brine ponds. We simulate such a scenario by specifying a 40 kilometer wide region of platform-top brine concentrated to halite saturation, either side of which salinity decreases linearly to that of normal seawater (36 ‰) over a distance of 10 kilometers (fig. 10). After 0.1 My, reflux from the isolated sub-basin drives flow both basinwards to discharge to the ocean and towards the platform interior where flow is forced to ascend and discharge through the platform-top by the right-side no-flow boundary (fig. 10A). In the absence of the right no-flow boundary, lateral flow would continue towards the right hand platform margin until the density gradient is exhausted. The total fluid flux, on the order of 10^5 kg/y/m, is the same magnitude as the previous halite brine example with a different platform-top salinity gradient (fig. 8E). The zone of highest fluid flux has however shifted towards the platform margin, reflecting the change in position of the maximum brine concentration (fig. 10). This change in position shuts off geothermal circulation at depth in the platform more effectively than when the maximum

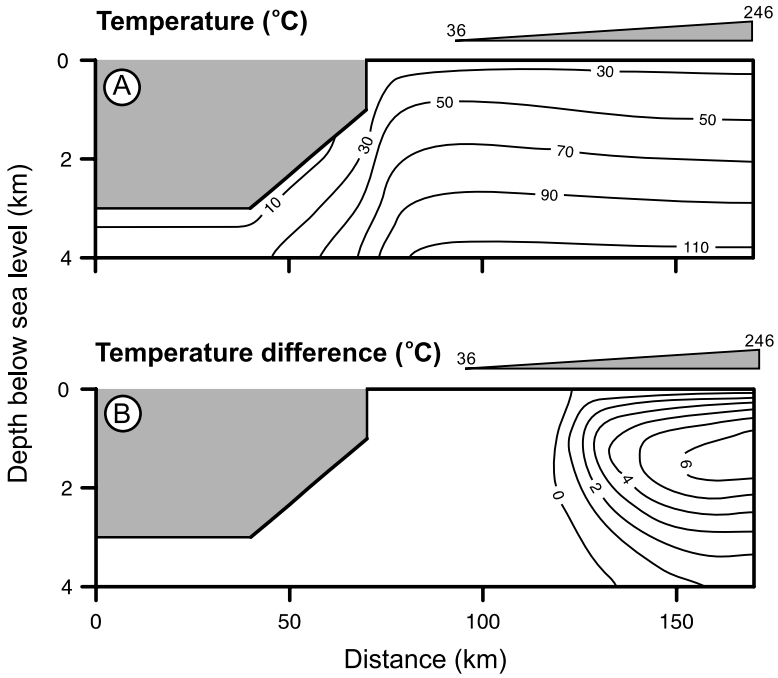

Fig. 9. Effect on temperatures of reflux circulation with brines concentrated up to halite saturation after 0.1 My. Temperature difference is relative to initial temperatures (fig. 5).

platform-top salinity is located further from the margin (compare figs. 8E and 10A). Note however that the salinity distribution (fig. 10B) indicates that the simple circulation indicated by the smoothed streamfuction plot is oversimplified. Two tongues of elevated salinity associated with the high flux zone to the left of the brine pool and the core of divergent flow system on the right are present, and are separated by a tongue of low salinity water. This indicates a convective upward circulation, the water from which is entrained in the seaward circulation cell, as indicated by the lower salinity of this plume despite its higher flux. In more complex brine distributions even more complex local circulation cells will likely become established. Thus both the brine concentration and its distribution across the platform-top are important controls on the style and extent of reflux and contemporaneous geothermal circulation.

Temporal changes of platform-top salinity.—The above simulations indicate how reflux could evolve if brine generating conditions persist for up to 1 My. However, changes in sea level will affect platform-top salinity and may stop reflux. Here we explore the fate of reflux brines in periods between intervals of active reflux. We simulate circulation of platform-top brines concentrated up to 150 permil for 0.1 My followed by an extended (10 My) period of platform drowning by seawater (fig. 11). The pattern and magnitude of reflux and geothermal circulation at 0.1 My are described above. When brine generating conditions cease, platform-top seawater is entrained by the continued movement of the brine plume generated by the previous period of active reflux, which as a consequence of its greater fluid density contrast continues to sink and disperse laterally (fig. 11C-H). We term this style of reflux circulation "latent reflux" (latent *sensu* hidden/concealed) to differentiate it from active reflux driven by brines on the platform-top (Jones and others, 2002). Latent reflux continues to entrain surficial seawater for at least 1 My, but by this time the total

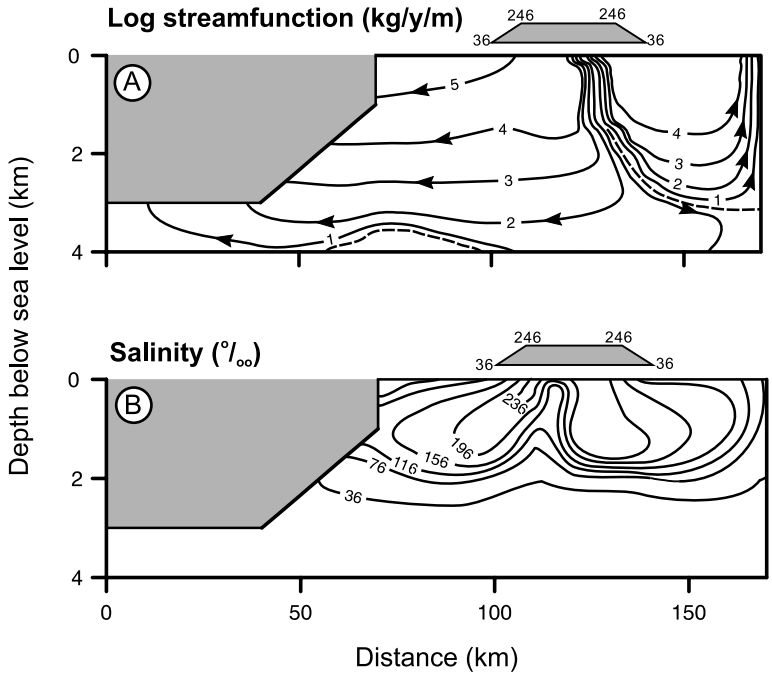

Fig. 10. Reflux from an isolated platform-top sub-basin, with brines concentrated up to halite saturation after 0.1 My.

fluid flux is an order of magnitude less than that for geothermal circulation at the margin (fig. 11E). After 10 My, extensive dilution of brines in the shallow (<0.5 km) subsurface reverses the fluid density gradient, and geothermal circulation now extends from the margin to the center of the platform in the upper 500 meters (fig. 11G and 11H). In the platform interior, beneath the upper zone of geothermal circulation, brines of reflux origin continue to circulate in a weak (on the order of 10^2 kg/y/m) convection cell. A second small convection cell, adjacent to the right side boundary, is geothermally-driven. Thus our simulations demonstrate that brines of reflux origin, originally concentrated up to gypsum saturation, can continue to affect patterns of fluid circulation up to 100 times the duration of a brine-forming event.

Reflux may be controlled by cyclic changes in relative sea level, which may be explained by eustatic, sedimentary and/or tectonic mechanisms (Read, 1995). To illustrate this effect we simulate a series of 0.1 My periods of platform-top brine generation (salinity 150 ‰) and active reflux, alternating with 0.1 My periods of platform-top flooding by normal seawater (salinity 36 ‰) with latent reflux, such as might occur during fourth order (eccentricity-driven) cyclicity. Because the time for brines to be flushed from the platform exceeds the frequency of reflux cyclicity, the resultant brine-driven circulation system (both active and latent reflux) affects a progressively greater proportion of the platform, with brines migrating towards the margin (fig. 12). Geothermal circulation is thus curtailed in terms of both the areal extent and magnitude of flux, discharge becoming initially confined to the margin of the platform (<0.4 My), and then progressively lower down the slope (>0.4 My), as in the earlier steady state circulations (fig. 7). Furthermore, the dilution of brines at shallow depth during latent reflux periods enhances flow during succeeding active

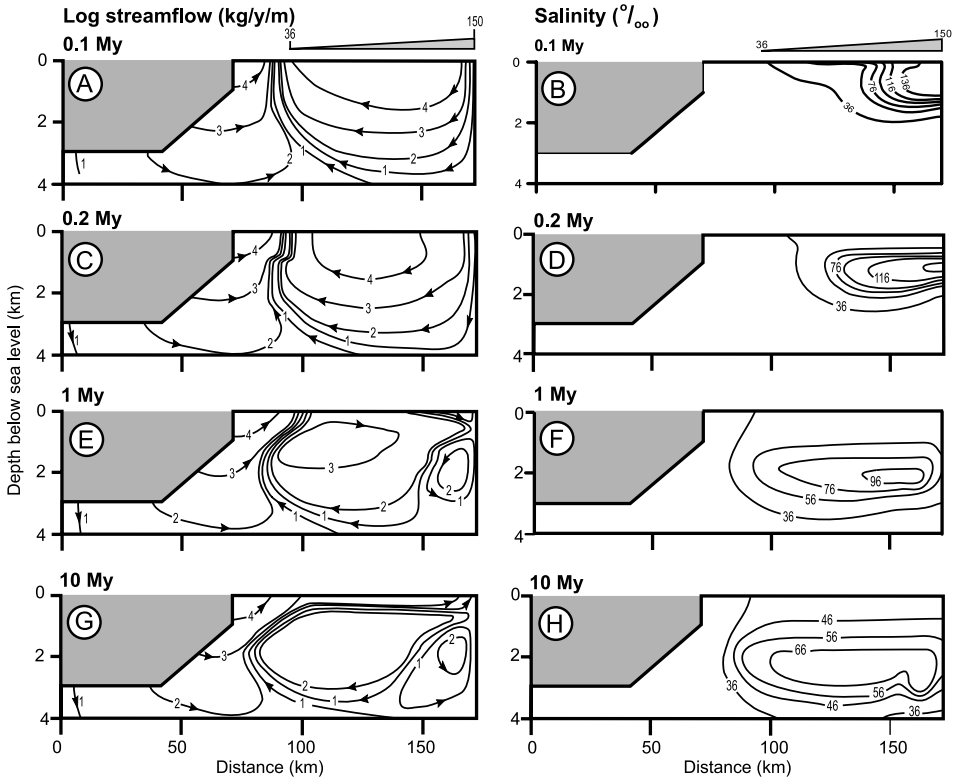

Fig. 11. Temporal evolution of groundwater circulation for up to 10 My after a single reflux event lasting 0.1 My with brines concentrated up to gypsum saturation.

reflux periods by increasing the shallow fluid density gradient when platform-top brine generating conditions resume (fig. 12).

Rock Properties

All investigations of the sensitivity of geothermal and reflux circulation to rock properties were undertaken using platform-top brines concentrated up to 246 permil as these generate distinct patterns of flow and plume characteristics within short simulated times (0.1 My). Additional simulations show that these results are comparable with those for lower salinity platform-top brines acting over longer times (Jones, ms, 2000). Results for rock properties are compared to our baseline simulation at a snapshot of 0.1 My (fig. 8E and 8F).

Porosity.—We examine the sensitivity of circulation to both a decrease and increase in porosity, for a given depth, by scaling our baseline curve by 0.8 and 1.2 respectively (fig. 3). This porosity range is similar to that measured by Schmoker and Halley (1982) at a particular depth. To isolate the effect of porosity, permeability was held at our baseline Class 2 curve (fig. 4). Although many parameters that control flow and transport are dependent on porosity (table 1), for the range tested porosity has a minor effect on fluid flux, but a significant effect on the rate of brine transport (fig. 13), because of the control on average linear velocity. The effects on salinity are most significant on the leading edge of the brine plume (fig. 13E and 13F), which advances less rapidly in the high porosity case than for the baseline simulation due to the greater

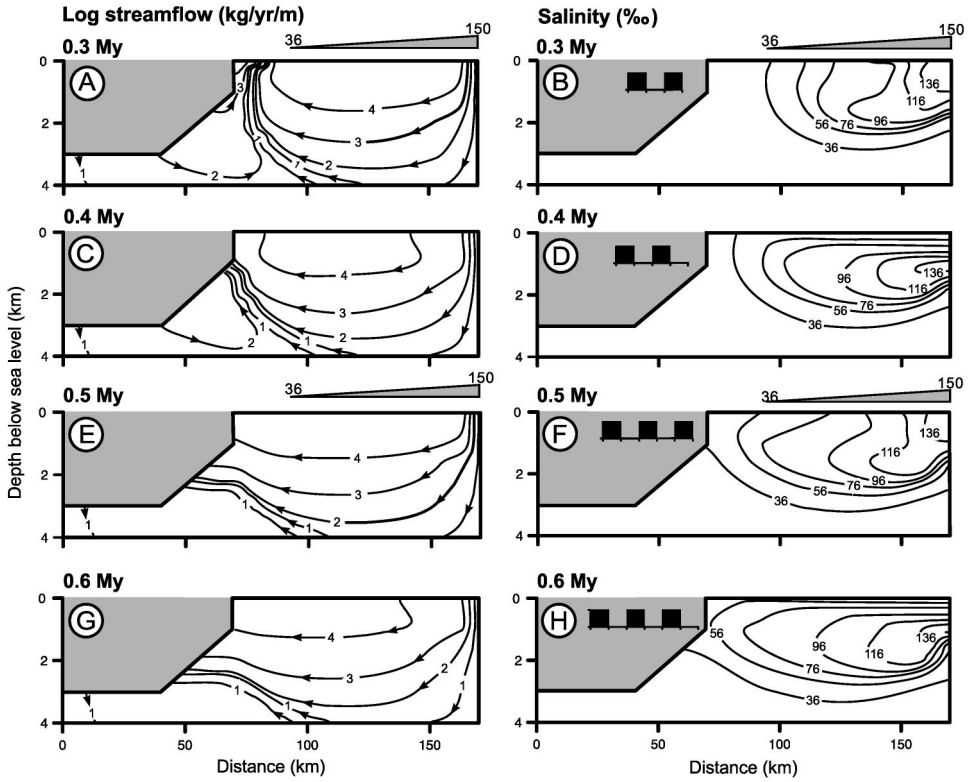

Fig. 12. Temporal evolution of groundwater circulation through a series of alternating 0.1 My periods of platform-top brines concentrated up to gypsum saturation (represented by the filled squares in the platform-top boundary condition history depicted in the ocean region) and unmodified seawater (represented by the line segment connecting the filled squares in the boundary condition history). For results at times earlier than 0.3 My see fig. 11 A to D.

volume of water that must be displaced. The reduced density contrast in the subsurface for the high porosity case reduces the impact on the platform margin geothermal circulation compared to the baseline, whereas for the low porosity case, this circulation is almost completely eliminated (as observed for the 1 My time step for the baseline simulation fig. 8G). With the higher porosities subsurface temperatures are higher (eqs 3 and 5), which enhances the fluid density gradient between platform-top waters and the underlying groundwater (eq 7), and also increases hydraulic conductivity (eqs 2 and 8). Compared to our baseline simulation this results in a 3 percent increase in the total fluid flux. In contrast, while the reduced temperatures for the low porosity case, reduce fluid flux in the platform 3 percent, this is less than the 20 percent increase in flow velocity due to the reduced porosity compared to our baseline simulation. Thus the plume extends both to greater depth and further out towards the margin for the low porosity case (fig. 13D and 13F).

Permeability.—We investigate the effect of permeability using the baseline porosity curve (fig. 3) and test the sensitivity of circulation for two additional permeability depth relationships, corresponding to a one order of magnitude increase and decrease in the Class 2 permeability for a given depth (fig. 4). Simulations where the entire platform permeability is specified using the Class 1 permeability depth curve (fig. 4) are numerically unstable, due to high Peclet Numbers, a common problem in

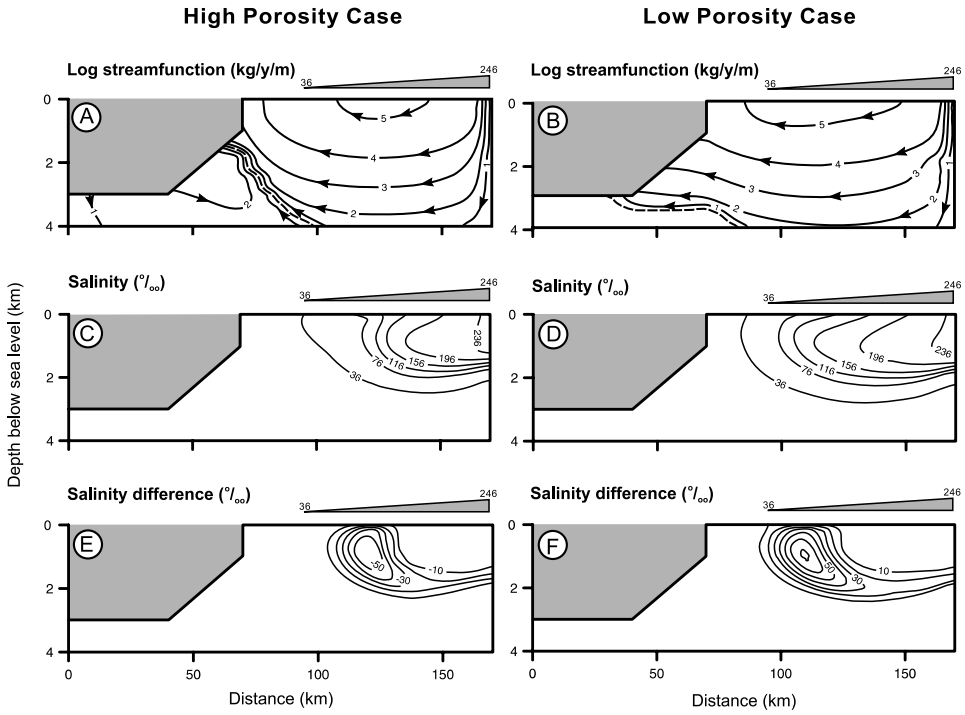

Fig. 13. Effect of carbonate porosity (fig. 3) on circulation after 0.1 My with platform-top brines concentrated up to halite saturation, for high porosity curve (fig. A, C and E) and low porosity curve (fig. B, D and F). Salinity difference is relative to our baseline simulation (fig. 8E, 8F).

simulating solute transport in very permeable (greater than 10^{-10} m^2) sediments (Ingebritsen and Sanford, 1998).

The permeability has a critical effect on the pattern and magnitude of flow, and the interaction between reflux and geothermal circulation (fig. 14). As would be expected from physical principles, the total fluid flux increases (decreases) by an order of magnitude for the high (low) permeability cases compared to the baseline case respectively. For the increased permeability case (fig. 14A and 14C), the circulation pattern and salinity distribution are equivalent to the baseline case after 1 My (fig. 8G and 8H), but with fluxes 10 times higher, giving rapid transport of brines from the platform interior to the platform margin. Similarly the low permeability case (fig. 14B and 14D) has a comparable circulation structure and salinity to the baseline case at 10 ky but lower fluxes (fig. 8C and 8D). For the high permeability case the enhanced fluid flux increases the advective heat transport, reducing the temperature by up to a maximum of 30 °C. In contrast, temperatures at the platform margin increase by a maximum of 20 °C as refluxing brines invade the margin and shut-off convective cooling of this region by geothermal circulation (Jones, ms, 2000; results not shown).

Permeability anisotropy.—Carbonate sequences with few or discontinuous low permeability layers or where sub-vertical fractures or karstic porosity are developed have less anisotropic permeability compared to our baseline simulation (anisotropy of 1000). Conversely, carbonate sequences with laterally extensive low permeability shale or evaporite layers can have a much higher permeability anisotropy. We simulate permeability anisotropies of 100 and 10,000 by respectively increasing and decreasing the vertical permeability by an order of magnitude. With a permeability anisotropy of 100

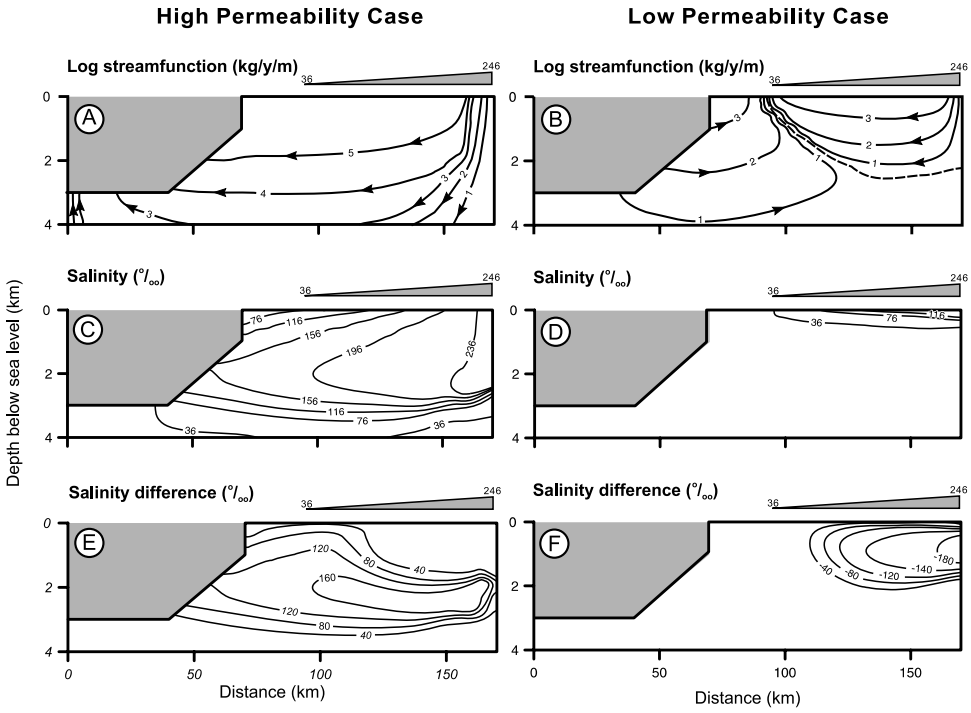

Fig. 14. Effect of permeability curve (fig. 4) on circulation after 0.1 My with platform-top brines concentrated up to halite saturation, for high permeability curve (fig. A, C and E) and low permeability curve (fig. B, D and F). Salinity difference is relative to our baseline simulation (fig. 8E, 8F).

the general pattern of reflux circulation after 0.1 My is similar to our baseline simulation (compare fig. 15A, 15C, 15E with fig. 8E and 8F), although there is an extension of the high fluid flux zone at shallow depth towards the platform margin, and fluxes at depth (>2 km) are significantly higher. However, the higher vertical permeability allows rapid descent of the brine plume and salinities are greater throughout the platform, particularly at depth and in the interior (fig. 15C and 15E). Note also the enhanced upward flow at the bank top towards the platform margin, indicated by the much stronger negative vertical salinity gradient in fig. 15C compared to fig. 8F. In contrast with a permeability anisotropy of 10,000 the pattern of circulation is radically different. After 0.1 My the reflux circulation is constrained within the upper 2 kilometers of the platform (fig. 15D and 15F), and below there is a weak geothermally driven circulation, which accounts for only 1 percent of the total fluid flux in the platform. The total fluid flux for the high anisotropy reflux circulation is an order of magnitude lower than for our baseline simulation (fig. 8E). This result is because of the reduced density contrasts that result from the much-reduced quantity of brine in the subsurface (fig. 15F) due to the lower vertical permeability. The shallow depth of circulation at 0.1 My also limits the depth of penetration of the brine plume.

Permeability: lateral variations:—We investigated the effect of lateral permeability variations on circulation in model aggrading and prograding platforms. Platforms aggrade where accommodation is generated by a rise in relative sea level resulting in a vertically stacked sequence of sedimentary units. Where accommodation is limited, excess sediment produced on the platform top is shed onto marginal slopes which prograde into the basin. Although diagenesis can significantly modify permeability we

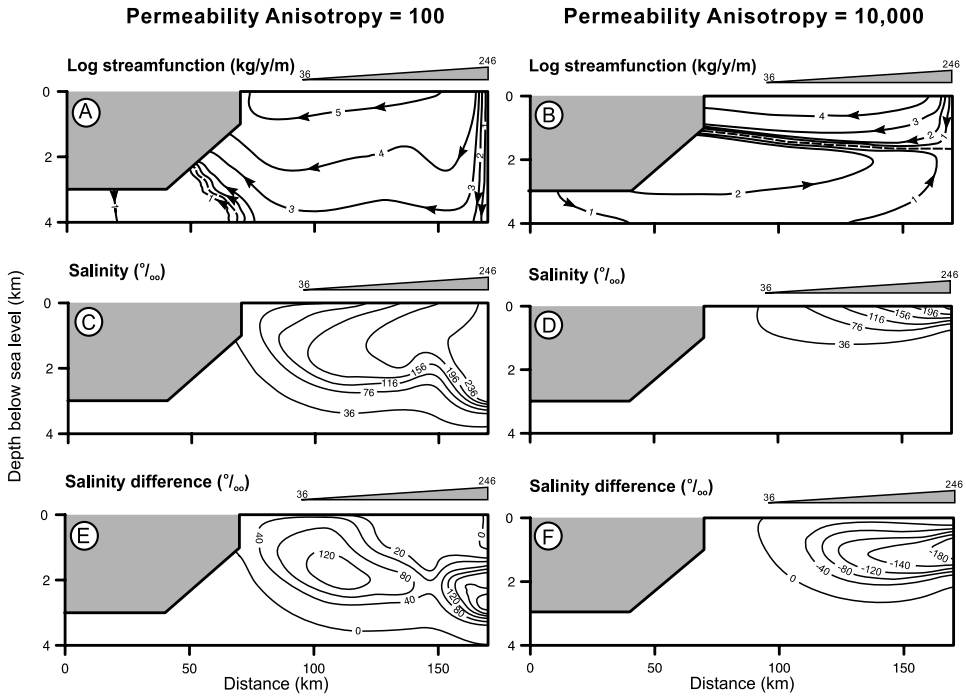

Fig. 15. Effect of permeability anisotropy on circulation after 0.1 My with platform-top brines concentrated up to halite saturation, for permeability anisotropy = 100 (fig. A, C and E) and permeability anisotropy = 10,000 (fig. B, D and F). Salinity difference is relative to our baseline simulation (fig. 8E, 8F).

assume that regional scale variations in permeability are simply controlled by the distribution of primary depositional facies. For our aggrading case we divide the platform laterally into four vertically continuous zones: basin, forereef slope, margin and shelf (fig. 16A), based on the idealized facies distribution for the Florida Shelf (Enos, 1977). For the basin we use the porosity-depth and porosity-permeability relationships developed by Harrison and Summa (1991) for Gulf of Mexico shales (figs. 3 and 4), and for all platform carbonates our baseline carbonate porosity curve (fig. 3). Permeability is then derived for the less permeable muddier forereef slope and shelf from the Class 2 (packstone facies) curve (fig. 4) and for the margin (which represents both the coral-algal reef and the associated fore / back reef rubble and sands) the Class 1 (grainstone facies) permeability curve, (fig. 4). Permeability anisotropy was the baseline value (1000) for all facies. In the aggrading platform scenario, reflux circulation dominates the broad shelf, but a strong geothermal circulation is established in the platform margin (fig. 16C). Because of the high permeability of the marginal facies, the geothermal circulation accounts for 99 percent of the total fluid flux, although the reflux circulation remains comparable in magnitude to that of the baseline simulation. The reflux circulation cell discharges in the vicinity of the boundary between the "shelf" and "margin" regions, landward of the geothermal cell. The lower head at depth in the high permeability platform margin compared to the baseline case, increases the extent of the lateral circulation of the reflux cell, resulting in a localized increase in salinity of up to 35 permil (fig. 16G) relative to our baseline simulation.

Reefs associated with prograding margins are a common feature in many carbonate platforms, for example the Upper Permian Capitan Platform (King, 1947) and the

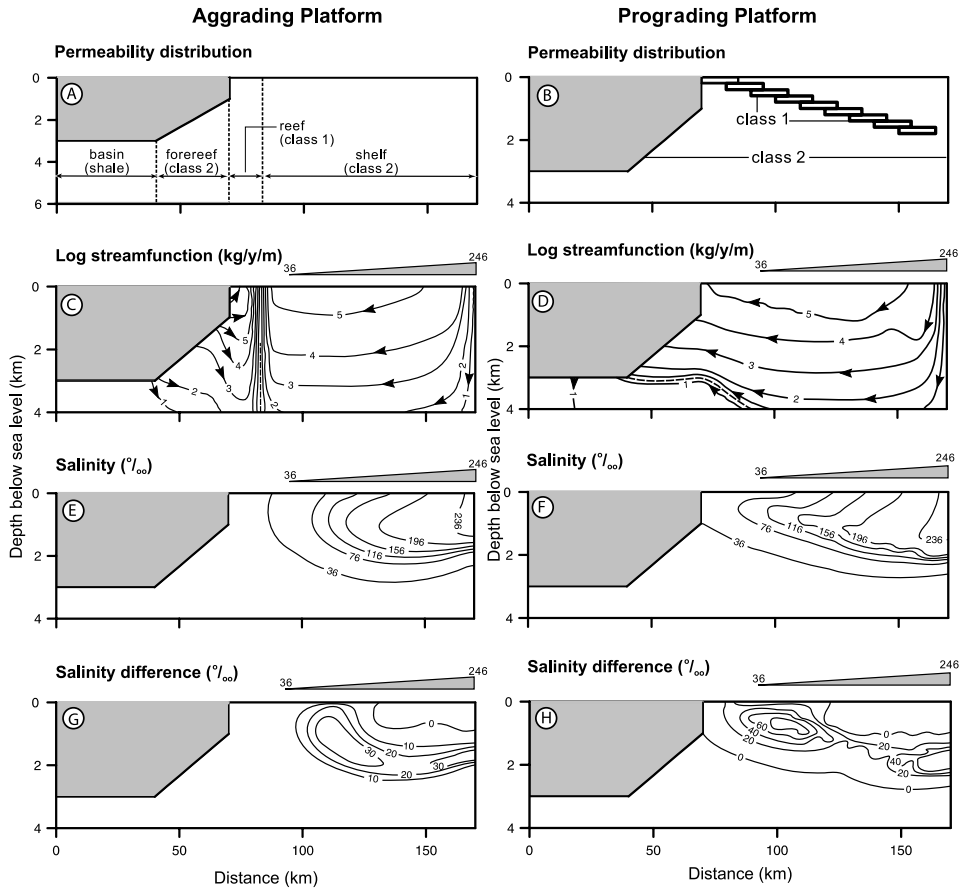

Fig. 16. Effect of platform permeability distribution on circulation after 0.1 My with platform-top brines concentrated up to halite saturation, for aggrading platform case (fig. A, C, E and G) and prograding platform case (fig. B, D, F and H). Salinity difference is relative to our baseline simulation (fig. 8E, 8F).

leeward margin of the Cenozoic Great Bahama Bank (Eberli and Ginsburg, 1987). Our prograding margin case is represented by a stacked series of progradational sequences 200 meters thick in the upper 1.6 kilometers of the platform, where each margin region has a width of 15 kilometers and a 5 kilometer overlap with under and overlying margin facies (fig. 16B). Porosity and permeability are calculated as above using the class 1 curve for the margin and class 2 for the other carbonates.

For the prograding platform, the hydraulic continuity of the high permeability marginal facies causes focusing of the reflux circulation (fig. 16F). After 0.1 My the total fluid flux (on the order of 10^5 kg/y/m) is much greater than in the baseline case, and is aligned along the axis of margin connectivity. It is also marked by a tongue of brine, which towards the platform margin is more than 80 ‰ more saline than the baseline simulation (fig. 16F and 16H). The majority (99 %) of the total fluid flux is driven by reflux, and this total is 2 orders of magnitude greater than our baseline simulation because of the more permeable marginal facies. In contrast to the aggradational case and despite the focussed fluid flux, the general style of circulation for the progradational simulation is very similar to that of the baseline case (compare figs. 8E and 16D), with almost complete shut-off of the geothermal circulation. There are

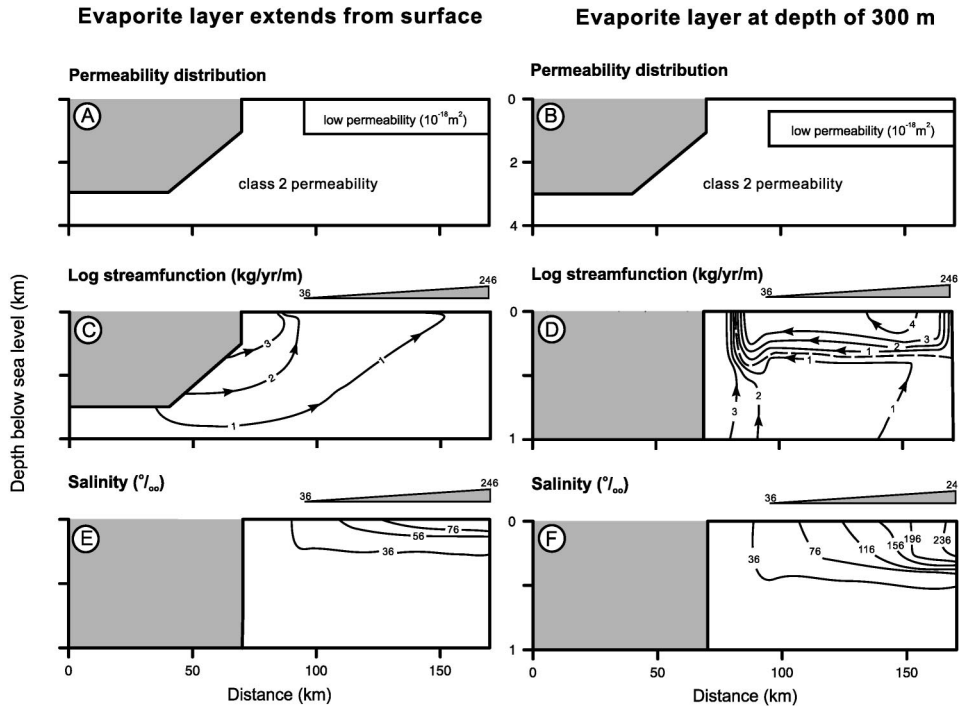

Fig. 17. Effect of low permeability layer on circulation after 0.1 My with platform-top brines concentrated up to halite saturation, for a layer extending 1000 m down from the platform-top (fig. A, C, and E) and for layer at a depth of 300 - 1300 m (fig. B, D and F). Note vertical scale is 1 km in figure C, E and F to display detail of reflux circulation and brine plume. The pattern and magnitude of circulation in figure C, at depths greater than 1 km, is similar to that in figure D.

however differences in salinity distribution (fig. 16H). By 0.1 My brines discharge to the ocean from the platform margin (especially in the shallowest marginal facies aggradational unit), and there is an increase in salinity at depth in the platform interior.

Permeability: low permeability layer.—Layers of low permeability rocks such as shales and evaporites have often been invoked to limit the extent of reflux circulation (see for example, Kendall, 1984; Machel and others, 1996; Tan and Mountjoy, 1998). At depths <1 kilometer the permeability of evaporites and shales (fig. 4) is at least 6 orders of magnitude less than that of carbonates at a comparable depth. We examine the effect of a 1 kilometer thick uniform low permeability (10^{-18} m^2) layer extending from the platform interior to 25 kilometers from the margin on circulation. Two scenarios are simulated using brines concentrated to halite saturation: (1) with the low permeability layer extending down from the platform-surface, to represent the shallow sealing of evaporites (fig. 17A), and (2) with the top of the low permeability layer at a depth of 300 meters (fig. 17B), the maximum depth evaporites remain relatively permeable (Sonnenfeld, 1984). Other rock parameters are based on the standard porosity depth curve, and class 2 permeability transformation as for the baseline case. With the low permeability layer at the platform surface, regional-scale reflux is almost completely suppressed (fig. 17A and 17C), and the geothermal circulation accounts for 94 percent of the total fluid flux. This circulation is however an order of magnitude weaker than in the non reflux simulation (fig. 5A) due to the reduced permeability in the interior. Brines extend less than 300 meters into the subsurface, and are both much more dilute

and more uniformly distributed laterally than in the baseline case (compare fig. 17E and 8F). Where the low permeability layer is in the subsurface, a limited reflux cell does develop in the carbonates above the low permeability unit (fig. 17D). However, as the total fluid flux is significantly less than in the baseline case, this is not sufficiently established to extend to the platform margin and cut-off the geothermal circulation, which is again an order of magnitude weaker than in the non-reflux case. The vertical development of the brine plume is restricted, with more rapid lateral transmission in the carbonates than vertically into the low permeability unit. Subsurface salinities are much higher than in the simulation with the low permeability unit at the surface (fig. 17E and 17F), maximum values being comparable to those in the baseline simulation (fig. 8F). In both cases the geothermal circulation is most active near the platform margin, with restricted circulation both below and within the low permeability layer (fig. 17C and 17D). Thus for both scenarios the presence of a low permeability layer has a significant effect on the pattern and magnitude of circulation after 0.1 My relative to our baseline simulation, but it is only when this unit is at the surface that the reflux circulation is almost totally retarded.

Dispersivity.—There is considerable uncertainty in the specification of dispersivity in regional-scale solute transport models (Steefel and Lasaga, 1994). We address this uncertainty by testing the sensitivity of reflux brine transport to variations in both the anisotropy and magnitude of dispersivity. Our sensitivity analysis results indicate that dispersivity is an important control on the shape and concentration of the brine plume (fig. 18). However, dispersivity is a relatively minor control on both the pattern and magnitude of circulation, which remains very similar to our baseline simulation (fig. 8E) for all dispersivity scenarios we test (Appold and Garven, 1999; Jones, ms, 2000).

Firstly we decrease our baseline dispersivity anisotropy of 10, (α_L=100 m and α_T =10 m) to 1 by increasing the vertical dispersivity to 100 meters (fig. 18A). Relative to the baseline distribution of salinity (fig. 8F) the increase in vertical dispersivity results in a more extensive but less concentrated brine plume, the leading edge of which extends to within 3 kilometers of the platform margin (fig. 18A). Because of enhanced vertical salt transport, concentrations are up to 30 permil lower at depths less than approximately 1 kilometer, and up to 70 permil higher at greater depths. Conversely a decrease in the vertical dispersivity to 1 meter, giving an increase in the dispersivity anisotropy to 100, reduces the rate of vertical plume extension (fig. 18B). This process results in reduction of brine concentration by up to 50 permil at depth, and maintenance of sharper salinity gradients at the base of the plume than for the baseline case (fig. 8F). Advective transport at shallow depth results in a brine plume that rises towards the platform margin, increasing salinity in leading edge of the plume by up to 70 permil (fig. 18B). Finally, we investigate the effect of maintaining, the dispersivity anisotropy at 10, but increasing both the horizontal and vertical dispersivity by an order of magnitude to 1000 and 100 meters respectively (fig. 18C). The higher dispersivities result in salinities up to 15 permil greater in the leading edge of the plume and significantly lower salinities (of up to 110 permil at the base of the plume) in the platform interior (fig. 18C). Overall the effect on brine plume shape is much less marked than for cases with a change in the dispersivity ratio. Parameterization of dispersivity in numerical models is poorly constrained, but our simulations show that the anisotropy of dispersivity is a significant control on regional-scale subsurface distribution of brine.

Platform Type

We have so far only considered simulations for rimmed shelves with relatively deep adjacent ocean basins. We now consider reflux circulation on distally steepened and homoclinal ramps, which are common platform morphologies in the geological record. The geometry and permeability distribution for our distally steepened and

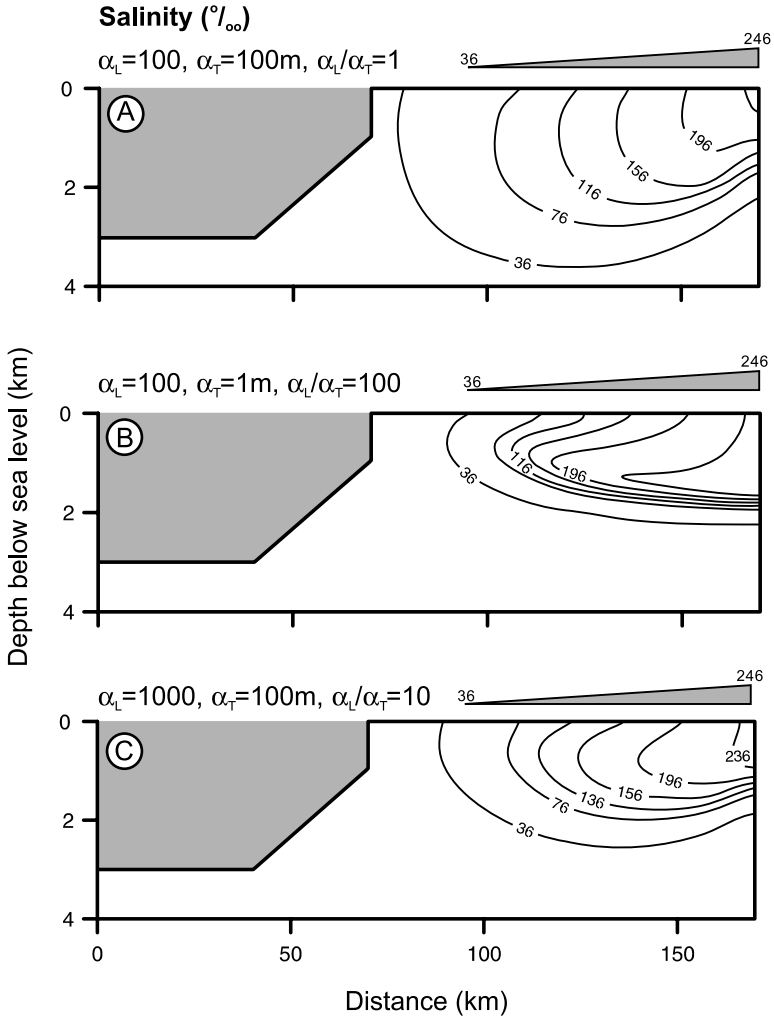

Fig. 18. Effect of dispersivity (anisotropy and magnitude) on the salinity distribution of the reflux brine plume, after 0.1 My with platform-top brines concentrated up to halite saturation. Figure A, horizontal dispersivity (α_L) =100 m, vertical dispersivity (α_T) =100 m, dispersivity anisotropy =1. Figure B, horizontal dispersivity (α_L) =100 m, vertical dispersivity (α_T) =1 m, dispersivity anisotropy =100. Figure C, horizontal dispersivity (α_L) =1000 m, vertical dispersivity (α_T) =100 m (dispersivity anisotropy =10).

homoclinal ramp simulations are depicted in fig. 19A and 19B respectively. In the distally steepened case the basin depth is 150 meters, with an abrupt transition to much shallower waters at 40 kilometers. The seafloor of the inner ramp has an angle of 0.003°. Inner ramp carbonates are simulated using the class 2 (packstone) porosity to permeability transformation, while for the muddier basin we employ the class 3 (mudstone) relationship (fig. 3). These relationships are also used for the inner and outer ramp respectively for the homoclinal ramp simulation. In this case the facies transition was set at 100 kilometers. The ramp surface was at a constant angle of 0.04°, and the maximum basin depth 150 meters. Note we have chosen to place the coast at the no-flow boundary to avoid inclusion of the complicating effects of meteoric

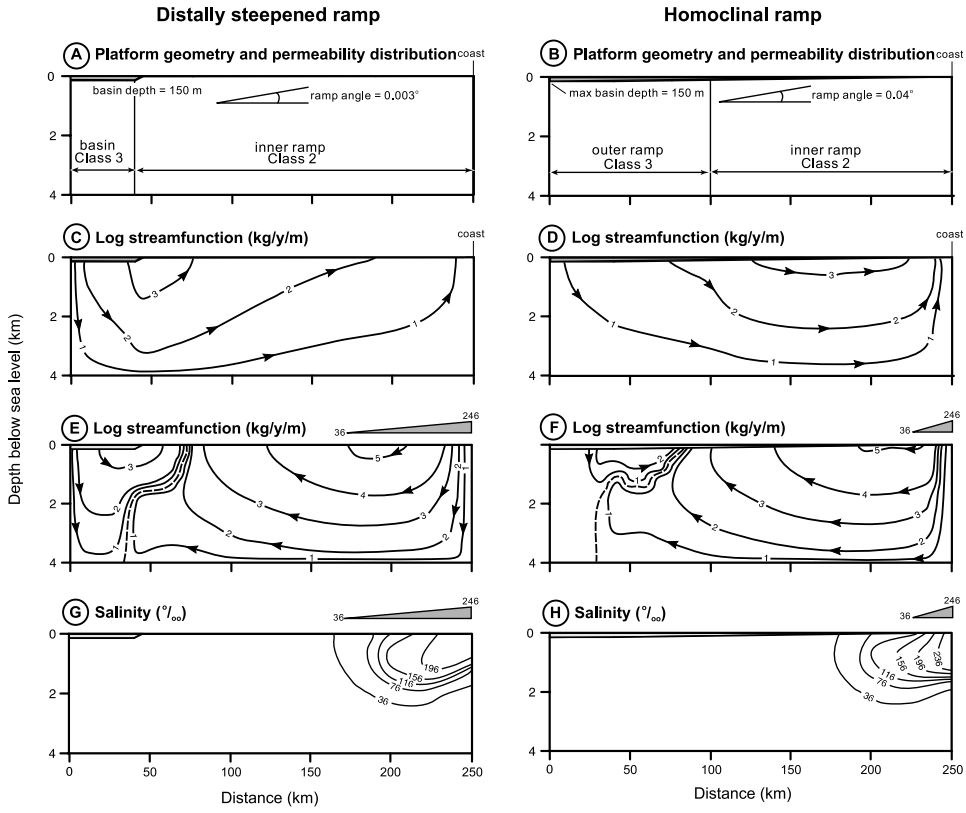

Fig. 19. Effect of platform geometry on circulation after 0.1 My with platform-top brines concentrated up to halite saturation, for a distally steepened ramp (fig. A, C, E and G) and a homoclinal ramp (fig. B, D, F and H). Note increased width of platform (250 km) and changes in the permeability and platform-top salinity distribution relative to our rimmed shelf case.

circulation derived from an exposed platform hinterland, which can significantly modify reflux circulation (Wood and others, 2002).

For platform-top waters specified as unmodified seawater (salinity 36 ‰), the steady state geothermal circulation is focused around the break in slope in the distally steepened ramp (fig. 19C), but also extends inland with discharge to the shallow waters overlying the platform. For the homoclinal ramp, fluxes are highest in the more permeable carbonates of the inner ramp (fig. 19D). In both these simulations the total fluid flux (on the order of 10^3 kg/y/m) is an order of magnitude less than geothermal circulation in a rimmed shelf platform (fig. 5). This result is due to the lower ocean-to-platform temperature contrasts for the shallow (150 m) specified basin depth (minimum ocean temperature 14 °C compared with 2 °C in the deep basin). We use these steady-state flow and temperature fields as the initial conditions for our simulations of reflux. As previously, we specify platform-top brines concentrated from seawater up to halite saturation (246 ‰).

For our distally steepened ramp simulation we specify a 75 kilometer region of platform-top brine (fig. 19E) based on the Jurassic Smackover platform (Moore and others, 1988). After 0.1 My, reflux circulation dominates the inner ramp region, while the geothermal circulation is restricted to 30 kilometers coastward from the distal break in slope (fig. 19E). Reflux generates a total fluid flux of about 10^5 kg/yr/m in

the inner ramp. This flux is 3 orders of magnitude greater than that of the previous geothermal circulation for this region, and is also 2 orders of magnitude stronger than the contemporary geothermal circulation adjacent to the distal shelf break (compare fig. 19C and 19E). Although brine is generated over little more than a third of the ramp, reflux drives basinward flow across much of the ramp, with discharge onto the ramp top (fig. 19E). After 0.1 My the brine plume is well developed, extending 80 kilometers horizontally and penetrating to a depth of 2 kilometers (fig. 19G).

In contrast to rimmed shelves and distally steepened ramps platform-top brine generation on homoclinal ramps is likely to be restricted to relatively narrow intratidal and supratidal zones (Burchette and Wright, 1992). Thus in our homoclinal ramp simulation we specify a 25 kilometer zone of platform-top brine adjacent to the coast (fig. 19F), based on the present-day Persian Gulf (Patterson and Kinsman, 1981). After 0.1 My, the circulation in the inner ramp is dominated by reflux, which also extends at depth to a substantial part of the outer ramp. The geothermal circulation is limited to the shallower part of the outer ramp (fig. 19F). The overall circulation pattern is comparable to that for the distally steepened ramp simulation, but is somewhat weaker in respect of reflux and particularly the geothermal circulation. The steeper salinity gradient specified for the platform-top brine (8.4 ‰/km) compared to that of our baseline simulation (2.8 ‰/km) and the distally steepened ramp (2.63 ‰/km), results in steeper density gradients between platform-top and underlying groundwaters. This process increases the rate of vertical plume development in the source area (fig. 19H), but the limited lateral extent of the zone of brine generation results in lower salinities in the subsurface in the distal parts of the plume.

DISCUSSION

Controls On the Style and Extent of Geothermal and Reflux Circulation

Our simulation results demonstrate the fundamental importance of considering the interaction between reflux and geothermal circulation, and provide general rules for understanding and predicting the occurrence of these two interacting flow systems. A critical aspect of our simulations is their demonstration of the evolution of reflux circulation as brines occupy more of the subsurface through time. At early stages, the extent of the reflux circulation cell is limited to the zone of maximum brine concentration with discharge upwards to the platform top, initially within the zone of lower brine concentration. Geothermal circulation is maintained at depth and dominant at the margin. With time reflux extends in both depth and lateral extent, with platform top discharge shifting towards the margin. For the majority of our simulations, the travel time of brines is much greater than that for establishment of the flow system. Thus the waters discharging from reflux-driven circulation are initially low salinity waters displaced from the interior by refluxing brines. The magnitude of fluid flux increases until circulation extends to discharge laterally from the platform margins, when geothermal convection is greatly reduced, then becomes restricted to the lower slope and eventually shuts off completely. Geothermal circulation can only operate where temperature induced fluid density gradients are not inverted by the presence of sub-surface brines. Our conclusion in part I that geothermal circulation in carbonate platforms should operate in carbonate platform whether the platform-top is flooded or emergent (Sanford and others, 1998) should be revised accordingly.

An important and previously unrecognized aspect of the time dependence of reflux circulation demonstrated by our modeling is that it continues even after brines are no longer present on the platform top. This result is significant because on flat-topped rimmed shelves quite small changes in relative sea level may terminate brine generation either by emergence, or flooding of the platform surface and submergence of the sill, which caused restriction. Our simulations demonstrate that

following even short periods (0.1 My) of active reflux of brines up to gypsum saturation, brines within the subsurface can continue to drive circulation in excess of 10 My. We term this variant 'latent reflux' (Jones and others, 2002) to distinguish it from previously recognized active reflux when brines are present on the platform-top, (Burchette and Wright, 1992; Whitaker and Smart, 1993). Importantly, the residence time of brines is much greater than that of astronomically-driven sea-level changes, and thus brines with a varying degree of dilution are likely to be a normal component of the groundwater system of many carbonate platforms. We suggest existing conceptual models be modified to incorporate the phenomena of latent reflux and its interaction with other groundwater circulation mechanisms.

The distribution and magnitude of permeability is a critical control on the balance between reflux and geothermal circulation, the magnitude of circulation and the geometry of the brine plume. As would be expected, the rate of evolution of both active and latent reflux systems is directly dependent upon the permeability of the platform carbonates. Similar flux and salinity distributions are predicted for active reflux simulations with an order of magnitude higher permeability in one tenth of the time. Permeability anisotropy has a major effect on the geometry of reflux circulation. Our simulations assume an apparently high anisotropy to represent the effect of sedimentary and diagenetic layering typically observed in platform carbonates. Reducing vertical permeability limits both the depth of brine penetration and the magnitude of flux at shallow depth. In contrast the depth penetration of brines is significantly enhanced by increasing the vertical permeability, giving more rapid elimination of geothermal circulation.

Spatial variations in permeability, which are typical of real platforms can significantly alter the pattern and magnitude of saline groundwater circulation. High permeability facies, such as characterize many platform margins, provide preferential flow routes that can act to focus refluxing brines. Our simulations also show that reflux brines that intersect highly permeable prograding units are channeled towards the platform margin, as envisaged in conceptual models that rely on permeable beds to explain the considerable distances between areas of brine recharge in the platform interior and dolomitized platform margins (Shields and Brady, 1995). However, the effectiveness of regions of elevated permeability to provide preferential flow routes for reflux will be critically dependent on: (1) their connectivity and (2) their location relative to regions of brine recharge on the platform-top.

Our simulations also demonstrate that units of low permeability severely retard reflux and that under such circumstances geothermal circulation can continue at depth in much of the platform. This behavior is of particular importance given the relatively low permeability of evaporite deposits that can form at the platform top from high salinity brines, which may mean that hypersaline reflux may be self-limiting. This result is consistent with the study of the MacLeod basin in Australia where low permeability evaporite beds prevent brines refluxing through the lagoon floor, but act to focus reflux at the lagoon edge (Logan, 1987). Ultimately the effect of evaporites on hypersaline reflux will depend on: (1) the rate of evaporite precipitation, the dynamics of which are strongly controlled by rates of brine leakage, including reflux (Sanford and Wood, 1991), (2) the stacking geometries of any subsurface evaporites relative to the location of brines on the active platform-top, and (3) the magnitude of evaporite permeability, which although very low for compacted evaporites is reported to be relatively high, (on the order of 10^{-11} m^2) prior to compaction and crystal annealing (Sonnenfeld, 1984).

We simulated the effect of relatively simple regional scale variations in permeability, but heterogeneity in the petrophysical properties of carbonate rocks exist at a range of smaller scales (Grant and others, 1994). These local heterogeneites can be a

trigger mechanism for brine fingering and impact the evolution of density driven flow systems like reflux (Schincariol, 1998; Jones and Xiao, 2004).

We have also considered the effects of variations in the salinity of platform-top brines. The salinity of platform top brines will directly control the rate at which the reflux is developed because fluid density, and thus the hydraulic head driving reflux, is primarily controlled by differences in fluid density determined by salinity. Our results confirm that higher salinity brines result in greater fluid flux, with more concentrated plumes that penetrate deeper and extend further towards the platform margin after the same interval of time. The dependence of the rate of extension of the circulation system on brine density is however nonlinear, being 100 times faster for a three times increase in maximum salinity (comparing brines up to gypsum saturation with mesohaline brines), but only 1000 times faster for a five times increase in maximum salinity (comparing brines up to halite saturation with mesohaline brines). Once the reflux circulation has been established, fluid fluxes are greater than for the preexisting geothermal circulation even for mesosaline brines, although this takes some 1 My under steady state boundary conditions. The demonstration that significant reflux circulation can occur even with mesosaline brines is important as conceptual models that invoke sub-hypersaline reflux are becoming increasingly popular (see for example, Melim, ms, 1991; Shields and Brady, 1995; Goldstein and others, 1998; Melim and Scholle, 2002). Such circulation will also not be limited by evaporite sealing, as is the case with higher salinity brines, and may have occurred in the past even where there is not specific geological evidence of its occurrence.

Our simulations have also investigated the effects of the extent and spatial distribution of platform-top brines. The simulations of localized brine pools on ramps and rimmed shelves show that the increased density gradients generated by a localized zone of high salinity give rise to higher salinities to greater depth in the subsurface than do more distributed sources. Circulation in the vicinity of the brine pool can also be quite complex, with local convective circulation of seawater displaced by brines. However, for a particular interval of time, more widely distributed brine sources give a greater quantity of brine and a wider extent of reflux circulation in the subsurface, together with a marginally higher fluid flux than do localized sources. The regional extent of the area of elevated salinity driving reflux circulation is therefore important.

We have focused on rimmed shelves for the majority of our simulations, but our results suggest that the generalizations above may also apply to ramp type platforms. Lateral fluid density contrasts between platform and ocean are lower on ramps than rimmed shelves due to warmer ocean temperatures in the shallower basin. Thus, the magnitude of fluid flux driven by geothermal circulation is an order of magnitude lower for ramps and distally steepened ramps than for our rimmed shelf simulations. This difference in flux is primarily because flow is not concentrated in the outer ramp where fluid density contrasts are greatest, but occurs in the more permeable inner ramp. Thus differences in circulation are both a function of platform geometry and facies controlled permeability variations. For ramps and distally steepened ramps, slightly elevated salinities are sufficient to offset the weak density gradients driving geothermal circulation and reflux will occur if platform-top waters become restricted. For brines of halite saturation, there is a rapid development of a deep and extensive reflux driven circulation in both the distally steepened and homoclinal ramp simulations, despite the much more limited area of brine generation in the latter. The reflux-driven circulation is two orders of magnitude stronger than that driven by geothermal circulation, and although not demonstrated in our limited duration experiments, the reflux circulation will probably eliminate the geothermal circulation throughout the platform, as was the case for rimmed shelves. Further simulations with mesohaline brines followed through time would be of considerable interest as the

extension of the reflux cell is much slower under these conditions. Although the zone of elevated subsurface salinities is of more limited extent for the homoclinal ramp than for the distally steeped ramp, migration of the zone of brine generation up and down the ramp, in response to relative sea level fluctuations (Burchette and Wright, 1992; Whitaker and Smart, 1993) would result in the widespread saturation of the ramp subsurface with reflux brines.

Finally, it is important to note that our simulations use linear (cartesian) coordinates to represent flow in a planar cross-section. This method assumes that the platform length perpendicular to the modeled cross section is significantly greater than the width of the section. This assumption is reasonable for the extensive rimmed shelves and ramps that we have modeled, which are frequently attached to a continental land mass. However, our results cannot be directly applied to small carbonate platforms, which occur often as circular atolls and would thus be better simulated using a radial or three-dimensional coordinate system. In such equidimensional platforms flow of refluxing brines would be expected to diverge as the cross-sectional area through which flow occurs increases towards the platform margins, as demonstrated for Enewetak Atoll by Jones and others (2000).

Numerical simulations of groundwater circulation in generic carbonate platforms provide important insights for process investigation, determining critical controls and developing general rules (Kaufman, 1994; Sanford and others, 1998; this study). However, considering the range of possible platform morphology and the combination of parameters that control geothermal and reflux circulation, many of which vary in time and space, predicting groundwater circulation in specific platforms from the geological record requires detailed specification of time variant rock properties and boundary conditions (Jones and others, 2000, 2003).

Implications for the Reflux Dolomitization Model

Reflux brines have the potential to generate secondary porosity by dissolving aragonite and calcite (Oswald and others, 1991; Sun, 1992), however the emphasis has been of their role in dolomitization. The Reflux Model has been widely advocated to explain dolomitization of carbonate platforms throughout the geological record, particularly those associated with evidence for hypersaline environments (Adams and Rhodes, 1960; Moore, and others, 1988; Jones and others, 2003). The major rationale for this model is that the circulation of brines provides the flux of magnesium critical for the dolomitization process (Land, 1985), although others have argued that the reduction of the kinetic barriers to dolomitization in brines compared to unaltered seawater is also important (Machel and Mountjoy, 1986). Our simulations thus provide a useful guide to the factors determining the distribution and extent of reflux circulation, and the groundwater flux critical for magnesium transport. Furthermore as they are physically-based they provide a much more reliable indication of the nature of reflux circulation than the cartoons often appended to studies of the fossil record, or of conceptual generalizations. For instance, while the earlier suggestions of Whitaker and Smart (1993) that reflux would be less important in ramps than in rimmed shelves is not confirmed by the results of our simulations.

By combining the distributions of fluid flux predicted in our simulations with magnesium mass balance calculations, crude spatial predictions of dolomite geobodies can be made (Wilson and others, 1990; Jones, ms, 2000; Jones and Rostron, 2000). Whilst these are again an improvement on previous conceptual (Whitaker and Smart, 1993) and analytical models (Shields and Brady, 1995), they do not incorporate feedbacks in permeability as a consequence of reactive transport, which can significantly impact the distribution of diagenesis (Ortoleva, 1994; Bolton and others, 1999). For example, the dolomitization of wackestones and mudstones can increase permeability by an order of magnitude (Lucia, 1995). In contrast, over-dolomitization where the

precipitation of dolomite cement occludes pore space can result in a severe permeability reduction of up to six orders of magnitude (Lucia and Major, 1994).

Such models assume that dolomitization is mass transport limited, but at present we have a very poor understanding of the kinetic controls on low-temperature dolomitization (Arvidson and Mackenzie, 1999), and it is uncertain whether dolomitization is kinetic or mass transport limited. Reactive transport models that couple fluid flow in carbonates platforms with geochemical reactions have the potential to realize more accurate predictions (Jones and others, 1997; Wilson and others, 2001; Jones and Xiao, 2004). For instance simulations of geothermal circulation by Wilson and others (2001) demonstrate that dolomitization is mass transport rather than rate limited, producing a well-defined reaction front. In the case of refluxing brines, the interplay between dolomitization, kinetics and mass transport is particularly challenging. For instance, reflux of high salinity brines (>150 ‰) is kinetically favorable to dolomitization because of the higher magnesium:calcium ratio following gypsum precipitation. However, as discussed above, the precipitation of low permeability evaporites can significantly curtail reflux, disrupting the simple dependence of fluid flux on platform-top salinity. Before we are able to resolve such issues by couple modeling, there is a need to improve specification of kinetic data for dolomitization at low temperature, and also to determine the effects of seed crystals and reactive surface area.

CONCLUSIONS

1. The three major controls on the relative magnitude and dynamic interaction between reflux and geothermal circulation are: (1) the concentration of brines on the platform-top, (2) the duration of brine generating conditions and (3) the permeability distribution. The extent and location of brine generating conditions on the platform-top are secondary controls.
2. The critical role of permeability is shown by comparison of our baseline permeability which shows platform-top brines concentrated up to 150 permil refluxing distances of 100 kilometers in 1 My, with comparable distance attained in as little as 0.1 My for an order of magnitude increase in permeability. In heterogeneous platforms, high permeability facies in hydraulic continuity act to focus refluxing brines and enhance brine transport.
3. Brines of reflux origin concentrated up to 150 permil have potentially long residence times of at least 100 times the duration of their formative reflux event and may be an important long-term control on geothermal and other groundwater circulation mechanisms.
4. Platform brines continue to sink and entrain surficial seawater when brine-generating conditions on the platform-top cease. We term this new variant of reflux circulation “latent-reflux”. Previous conceptual models of groundwater circulation in carbonate platforms should be revised to incorporate this new process of latent-reflux, which may deliver a significant quantity of dissolved reactants, for example magnesium for dolomitization.
5. Reflux circulation should also be important in carbonate ramps. Even slightly elevated salinites at the top of the inner ramp are sufficient to offset the weak density gradients that drive geothermal circulation in this type of platform.
6. The combination of parameters which primarily control the dynamic interaction between reflux and geothermal circulation, many of which vary both in time and space, result in complex patterns of fluid flow and brine transport. Considering our uncertainty in the magnitude and distribution of permeability it will be difficult to accurately predict circulation in modern platforms and even more challenging in ancient platforms. However, our simulations investigate process, determine the general constraints and identify the critical parameters that control reflux and its interaction with geothermal circulation.

ACKNOWLEDGMENTS

This study forms part of G. D. Jones Ph.D. thesis funded by a University of Bristol scholarship. Ben Rostron and Ward Sanford funded additional periods of study at the University of Alberta and the United States Geological Survey, respectively. We thank Grant Garven and Craig Simmons for insightful reviews. Drew Ellis (University of Bristol) and Laura Parnell (ExxonMobil) provided cartographic assistance.

References

Adams, J. E., and Rhodes, M. L., 1960, Dolomitization by seepage reflux: American Association of Petroleum Geologists Bulletin, v. 44, p. 1912-1920.

Adams, J. J., and Bachu, S., 2002, Equations of state for basin geofluids: algorithm review and intercomparison for brines: Geofluids, v. 2, p. 257-271.

Amthor, J. E., Mountjoy, E. W., and Machel, H. G., 1994, Regional scale porosity and permeability variations in upper Devonian Leduc buildups, implications for reservoir development and prediction in carbonates: American Association of Petroleum Geologists Bulletin, v. 78, p. 1541-1559.

Appold, M. S., and Garven, G., 1999, The hydrology of ore formation in the southeast Missouri district: numerical models of topography driven fluid flow during the Ouachita Orogeny: Economic Geology, v. 94, p. 913-936.

Arvidson, R. S., and Mackenzie, F. T., 1999, The dolomite problem: control of precipitation kinetics by temperature and saturation state: American Journal of Science, v. 299, p. 257-288.

Bethke, C. M., Lee, M. K., and Park, J., 1999, Basin Modeling with Basin2 release 4.1: University of Illinois, Hydrogeology Program, 213 p.

Bolton, E. W., Lasaga, A. C., and Rye, D. M., 1999, Long-term flow/chemistry feedback in a porous medium with a heterogeneous permeability: kinetic control of dissolution and precipitation: American Journal of Science, v. 299, p. 1-68.

Burchette, T. P., and Wright, V. P., 1992, Carbonate ramp depositional systems: Sedimentary Geology, v. 79, p. 3-57.

Busby, R. F., and Dick, G. F., 1964, Oceanography of the eastern Great Bahama Bank, part I, temperature – salinity distribution: United States Naval Oceanographic office, 42 p.

Diersch, H. J. G., and Kolditz, O., 2002, Variable-density flow and transport in porous media: approaches and challenges: Advances in Water Resources, v. 25, p. 899-944.

Eberli, G. P., and Ginsburg, R. N., 1987, Segmentation and coalescence of Cenozoic carbonate platforms, northwestern Great Bahama Bank: Geology, v. 15, p. 363-388.

Enos, P., 1977, Holocene sediment accumulations of South Florida: Memoirs of the Geological Society of America, v. 147, p. 1-130.

Evans, D. G., and Nunn, J. A., 1989, Free thermohaline convection in sediments surrounding a salt column: Journal of Geophysical Research, v. 94B, p. 12413-12422.

Evans, D. G., and Raffensperger, J. P., 1992, On the stream function for variable-density groundwater flow: Water Resources Research, v. 28, p. 2141-2145.

Fan, Y., Duffy, C. J., and Oliver, D. S., Jr., 1997, Density-driven groundwater flow beneath closed desert basins; field investigations and numerical experiments: Journal of Hydrology, v. 196, p. 139-184.

Fisher, W. L., and Rodda, P. U., 1969, Edwards Formation (Lower Cretaceous), Texas: dolomitization in a carbonate platform system: American Association of Petroleum Geologists Bulletin, v. 53, p. 55-72.

Gelhar, L. W., 1986, Stochastic subsurface hydrology from theory to applications: Water Resources Research, v. 22, p. 135-145.

Goldstein, R. H., Banner, J. L., Kwong, M. H., Luczaj, J. A., Ward, W. B., and Westphal, H., 1998, Importance of brine reflux in diagenesis: Fluid flow in carbonates: interdisciplinary approaches: Egg Harbor, Wisconsin, SEPM research conference: Fluid flow in Carbonates, program with abstracts.

Grant, C. W., Goggin, D. J., and Harris, P. M., 1994, Outcrop analog for cyclic-shelf reservoirs, San Andres Formation of Permian Basin: stratigraphic framework, permeability distribution, geostatistics and fluid flow modeling: American Association of Petroleum Geologists Bulletin, v. 78, p. 23-54.

Griffen, G. M., Reel, D. A., and Pratt, R. W., 1977, Heat flow in Florida oil test holes and indications of oceanic crust beneath the South Florida-Bahamas platform, *in* Smith, D. L., and Griffen, G. M., editors, The geothermal nature of the Florida plateau: State of Florida Department of Natural Resources, Special Publication, n. 21, p. 43-63.

Hanor, J. S., 1987, Kilometre-scale thermohaline overturn of pore waters in the Louisiana Gulf Coast: Nature, v. 327, p. 501-503.

Harrison, W. J., and Summa, L. L., 1991: Paleohydrology of the Gulf of Mexico Basin: American Journal of Science, v. 291, p. 109-176.

Hsu, K. J., and Siegenthlaer, C., 1969, Preliminary experiments on hydrodynamic movements induced by evaporation and their bearing on the dolomite problem: Sedimentology, v. 12, p. 11-25.

Ingebritsen, S. E., and Sanford, W. E., 1998, Groundwater in geologic processes: Cambridge, Cambridge University Press, 341 p.

Jones, G. D., ms, 2000, Numerical modelling of saline groundwater circulation in carbonate platforms: Ph.D. thesis, University of Bristol, United Kingdom, 330 p.

——— 2003, New Insights for predicting reflux dolomite geobodies (abstract): 12th Bathurst Meeting International Conference of Carbonate Sedimentologists, p. 51.

Jones, G. D., and Rostron, B. J., 2000, Analysis of fluid flow constraints in regional-scale reflux dolomitization: constant versus variable-flux hydrogeological models: Bulletin of Canadian Petroleum Geology, v. 48, p. 230-245.
Jones, G. D., and Xiao, Y., 2004, Reflux dolomitization and porosity evolution: insights from reactive transport models, *in* Davies, G., and Packard, J., editors, Dolomites the spectrum – mechanisms models, reservoir development: Canadian Society of Petroleum Geologists (extended abstract).
Jones, G. D., Whitaker, F. F., Smart P. L., and Sanford, W. E., 1997, Dolomitization of carbonate platforms by saline groundwater: Coupled numerical modelling of thermal and reflux circulation mechanisms, *in* J. Hendry, P. Carey, J. Parnell, A. Ruffell, and R. Worden, editors: Belfast, The Queens' University, Proceedings of Geofluids II Conference, p. 378-381.
——— 1998, The critical role of porosity / permeability transformations for modelling regional groundwater circulation in carbonate rocks (abstract): Door County, Wisconsin, SEPM Research Conference, Fluid Flow in Carbonates: Interdisciplinary Approaches, program with abstracts.
——— 2000, Numerical modeling of geothermal and reflux circulation in Enewetak Atoll: Implications for dolomitization: Journal of Geochemical Exploration, v. 69-70, p. 71-75.
——— 2002, Fate of reflux brines in carbonate platforms: Geology, v. 30, p. 371-374.
Jones, G. D., Smart, P. L., Whitaker, F. F., Rostron, B. J., and Machel, H. G., 2003, Numerical modeling of reflux dolomitization in the Grosmont platform complex (Upper Devonian), Western Canada Sedimentary Basin: American Association of Petroleum Geologists Bulletin, v. 87, p. 1273-1298.
Juster, T., Kramer, P. A., Vacher, H. L., Swart, P. K., and Stewart, M., 1997, Groundwater flow beneath a hypersaline pond, Cluett Key, Florida Bay, Florida: Journal of Hydrology, v. 197, p. 339-369.
Kaufman, J. K., 1994, Numerical models of fluid flow in carbonate platforms: implications for dolomitization: Journal of Sedimentary Research, v. A64, p. 128-139.
Kendall, A. C., 1984, Origin and geometry of Red River dolomite reservoirs, Western Williston Basin: Discussion: American Association of Petroleum Geologists Bulletin, v. 68, p. 776-784.
King, R. H., 1947, Sedimentation in Permian Castile Sea: American Association of Petroleum Geologists Bulletin, v. 31, p. 470-477.
Klotz, D., Seiler, H., Moser, H., and Neumaier, F., 1980, Dispersivity and velocity relationships from laboratory and field relationships: Journal of Hydrology, v. 45, p. 169-184.
Land, L. S., 1985, The origin of massive dolomite: Journal of Geological Education, v. 33, p. 112-125.
Logan, B. W., 1987, The MacLeod evaporite basin, Western Australia: American Association of Petroleum Geologists Memoirs, v. 44, 140 p.
Lucia, F. J., 1995, Rock fabric / petrophysical classification of carbonate pore space for reservoir characterization: American Association of Petroleum Geologists Bulletin, v. 79, p. 1275-1300.
Lucia, F. J., and Major, R. P., 1994, Porosity evolution through hypersaline reflux dolomitization, *in* Purser, B., Tucker, M., and Zenger, D., editors, Dolomites: International Association of Sedimentologists Special Publication 21, p. 345-360.
Lyons, W. B., Tyler, S. W., Gaudette, H. E., and Long, D. T., 1995, The use of strontium isotopes in determining groundwater mixing and brine fingering in a playa spring zone, Lake Tyrrell, Australia: Journal of Hydrology, v. 167, p. 225-239.
Machel, H. G., and Mountjoy, E. W., 1986, Chemistry and environments of dolomitization - a reappraisal: Earth Science Reviews, v. 23, p. 175-222.
Machel, H. G., Mountjoy, E. W., and Amthor, J. E., 1996, Discussion: Mass balance and fluid flow constraints on regional scale dolomitization, late Devonian, Western Canada Sedimentary Basin: Bulletin of Canadian Petroleum Geology, v. 44, p. 566-571.
Melim, L. A., ms. 1991, The origin of dolomite in the Permian (Guadalupian) Capitan Formation, Delaware Basin, West Texas and New Mexico: Implications for dolomitization models: Ph.D. thesis, Southern Methodist University, Dallas, Texas, 387 p.
Melim, L. A., and Scholle, P. A., 2002, Dolomitization of the Capitan Formation forereef facies (Permian, West Texas and New Mexico): seepage reflux revisited: Sedimentology, v. 49, p. 1207-1227.
Meyers B. J., Lu, F. H., and Zachariah, J. K., 1997, Dolomitization by mixed evaporative brines and freshwater, Upper Miocene carbonates, Spain: Journal of Sedimentary Research, v. 67, p. 898-912.
Moore, C. H., Chowdhury, A., and Chan, L., 1988, Upper Jurassic Smackover platform dolomitization, northwestern Gulf of Mexico: a tale of two waters, *in* Sukloa, V., and Baker, P. A., editors, Sedimentology and Geochemistry of Dolostones: SEPM Special Publication, n. 43, p. 175-189.
Mresah, M. H., 1998, The massive dolomitization of platformal and basinal sequences: proposed models from the Paleocene, Northeast Sirte Basin, Libya: Sedimentary Geology, v. 116, p. 199-226.
Muldoon, M. A., Simo, J. A., and Bradbury, K. R., 1998, Tracer study for characterization of groundwater movement and contaminant transport in a fractured dolomite aquifer: Wisconsin Geological and Natural History Open File Report, WOFR 1998-2, 45 p.
Nield, D., 1968, Onset of thermohaline convection in a porous medium: Water Resources Research, v. 4, p. 553-560.
Oberdorfer, J. A., and Buddemeier, R. W., 1988, Climate change: effects on reef island resources: Australia, Proceedings of the 6th International Coral Reef Symposium, v. 3, p. 523-527.
Ophori, D. U., 1998, The significance of viscosity in density-dependent flow of groundwater: Journal of Hydrology v. 204, p. 261-270.
Ortoleva, P. J., 1994, Geochemical self-organization: Oxford, Oxford University Press, 411 p.
Oswald, E. J., Schoonen, M. A. A., Meyers, W. J., 1991, Dolomitization in seas in evaporitic basins: a model for pervasive dolomitization of upper Miocene reefal carbonates in the western Mediterranean (abstract): American Association of Petroleum Geologists Bulletin, v. 75, p. 649.
Patterson, R. J., and Kinsman, D. J. J., 1981, Hydrologic framework of a sabkha along the Arabian (Persian) Gulf: American Association of Petroleum Geologists Bulletin, v. 66, p. 28-43.

Perkins, R. D., Dwyer, G. S., Rosoff, D. B., Fuller, J., Baker, P. A., and Lloyd, R. M., 1994, Salina sedimentation and diagenesis; West Caicos Island, British West Indies, *in* Purser, B., Tucker, M., and Zenger, D., editors, Dolomites: International Association of Sedimentologists Special Publication 21, p. 37-54.

Phillips, O. M., 1991, Flow and Reactions in Permeable Rocks: Cambridge, Cambridge University Press, 285 p.

Pomar, L., and Ward, W. C., 1999, Reservoir-scale heterogeneity in depositional packages and diagenetic patterns on a reef rimmed platform, Upper Miocene, Mallorca, Spain: Association of Petroleum Geologists Bulletin, v. 83, p. 1759-1773.

Purser, B. H., 1973, The Persian Gulf: Berlin, Springer-Verlag, 471 p.

Read, J. F., 1995, Overview of carbonate platform sequences, cycle stratigraphy and reservoirs in greenhouse and ice-house worlds in Read, J. F., Kerans, C., Webber, L. J., Sarg, J. F., and Wright, F. M., editors, Milankovitch sea-level changes, cycles and reservoirs on carbonate platforms in greenhouse and ice-house worlds: SEPM short course 35, 183 p.

Robinson, R. A., and Stokes, R. H., 1965, Electrolyte solutions: London, Butterworths Press, 571 p.

Rovey, C. W., and Cherkauer, D. S., 1995, Scale dependency of hydraulic conductivity measurements: Ground Water, v. 33, p. 769-780.

Saller, A. H., and Henderson, N., 1998, Distribution of porosity and permeability in platform dolomites: insight from the Permian of west Texas: American Association of Petroleum Geologists Bulletin, v. 82, p. 1528-1550.

Sanford, W. E., and Wood, W. W., 1991, Brine evolution and mineral deposition in hydrologically open evaporite basins: American Journal of Science, v. 291, p. 687-710.

Sanford, W. E., Whitaker, F. F., Smart, P. L., and Jones, G. D., 1998: Numerical Analysis of seawater circulation in carbonate platforms: I geothermal circulation: American Journal of Science, v. 298, p. 801-828.

Sarkar, J., Nunn, J. A., and Hanor, S., 1995, Free thermohaline convection beneath allochthonous salt sheets: an agent for salt dissolution and fluid flow in Gulf Coast sediments: Journal of Geophysical Research, v. 100 B9, p. 18085-18092.

Schincariol, R. A., 1998, Dispersive mixing dynamics of dense miscible plumes: natural perturbation initiation by local-scale heterogeneities: Journal of Contaminant Hydrology, v. 34, p. 247-271.

Schmoker, J. W., and Halley, R. B., 1982, Carbonate porosity versus depth: a predictable relation for South Florida: Association of Petroleum Geologists Bulletin, v. 66, p. 2561-2570.

Scruton, P. S., 1953, Deposition of evaporites: American Association of Petroleum Geologists Bulletin, v. 37, p. 2498-2512.

Sharp, J. M., Fenstemaker, T. R., Simmons, C. T., McKenna, T. E., and Dickinson, J. K., 2001, Potential salinity driven free convection in a shale-rich sedimentary basin: Example from the Gulf of Mexico basin in south Texas: American Association of Petroleum Geologists Bulletin, v. 85, p. 2089-2110.

Shields, M. J., and Brady, P. V., 1995, Mass balance and fluid flow constraints on regional scale dolomitization, late Devonian, Western Canada Sedimentary Basin: Bulletin of Canadian Petroleum Geology, v. 43, p. 371-392.

Simmons, C. T., and Narayan, K. A., 1997, Mixed convection processes beneath a saline disposal basin: Journal of Hydrology, v. 194, p. 263-285.

Simmons, C. T., Fenstemaker, T. R., and Sharp, J. M., Jr., 2001, Variable-density groundwater flow and solute transport in heterogeneous porous media: approaches, resolutions and future challenges: Journal of Contaminant Hydrology, v. 52, p. 245-275.

Simms, M. A., 1984, Dolomitization by groundwater flow systems in carbonate platforms: Transactions of the Gulf Coast Association of Geological Sciences, v. 24, p. 411-420.

Sonnenfeld, P., 1984, Brines and evaporates: Orlando, Academic Press, 313 p.

Steefel, C. I., and Lasaga, A. C., 1994, Putting transport in water rock interaction models: Geology, v. 20, p. 680-684.

Sun, S. Q., 1992, Skeletal aragonite dissolution from hypersaline seawater a hypothesis: Sedimentary Geology, v. 77, p. 249-257.

Switzer, S. B., Holland, W. G., Christie, D. S., Graf, C. G., Hedinger, A. S., McAuley, R. J., Wierzicki, R. A., and Packard, J. J., 1994, Devonian Woodbend - Winterburn strata of the Western Canada Sedimentary Basin, *in* Mossop, G. D., and Shetsen, I., editors, Geological Atlas of the Western Canada Sedimentary Basin: Canadian Society of Petroleum Geologists and Alberta Research Council, p. 165-202.

Tan, W., and Mountjoy, E. W., 1998, Limited reflux dolomitization in restricted Upper Devonain carbonate evaporated shelves, southeastern Alberta: Alicante, Spain, International Association of Sedimentologists, 15th International Sedimentological Congress, Abstracts, p. 754-755.

Tator, B. A., and Hatfield, L. E., 1975, Bahamas present complex geology: Oil and Gas Journal, v. 73, p. 172-176.

Traverse, A., and Ginsburg, R. N., 1966, Palynology of the surface sediments of the Great Bahama Bank as related to water movement and sedimentation: Marine Geology, v. 4, p. 417-459.

Uwiera, M., ms, 1998, Numerical simulation of brine migration in the vicinity of a potash mine: MSc. Thesis, University of Saskatchewan, Canada, 208 p.

Voss, C., 1984, SUTRA - saturated unsaturated transport - A finite element simulation model for saturated unsaturated fluid density dependent groundwater flow with energy transport and chemically-reactive single species transport: U.S. Geological Survey Water Resources Investigative Report 84-4369, 409 p.

Whitaker, F. F., and Smart, P. L., 1990, Circulation of saline groundwaters through carbonate platforms: evidence from the great Bahama Bank: Geology, v. 18, p. 200-204.

——— 1993, Circulation of saline groundwaters in carbonate platforms: a review and case study from the Bahamas, *in* Horbury, A. D., and Robinson, A. G., editors, Diagenesis and Basin Development: American Association of Petroleum Geologists Studies in Geology, v. 36, p. 113-134.

——— 1997, Hydrology and hydrogeology of the Bahamian Archipelago: Developments in Sedimentology 54, p. 183-216.
Whitaker, F. F., Smart, P. L., Vahrenkamp, V. C., Nicholson, H., and Wogelius, R., 1994, Dolomitization by near-normal sea-water? Field evidence from the Bahamas, *in* Purser, B., Tucker, M., and Zenger, D., editors, Dolomites: International Association of Sedimentologists Special Publication 21, p. 111-132.
Whitaker, F. F., Smart, P. L., and Jones, G. D., 2004, Dolomitization: from conceptual to numerical models, *in* Braithwaite, C., Rizzi, G., and Darke, G., editors, The geometry and Petrogenesis of Dolomite Hydrocarbon Reservoirs: Special Publication of the Geological Society of London.
Wilson, A. M., Sanford, W. E., Whitaker, F. F., and Smart, P. L., 2001, Spatial patterns of diagenesis during geothermal circulation in carbonate platforms: American Journal of Science, v. 301, p. 727-752.
Wilson, E. N., Hardie, L. A., and Phillips, O. M., 1990, Dolomitization front geometry, fluid flow patterns, and the origin of dolomite: the Triassic Latemar Buildup, northern Italy: American Journal of Science, v. 290, p. 741-796.
Wood, W. W., Sanford, W. E., and Habshi, A. R. S. A., 2002, Source of solutes to the coastal sabkha of Abu Dhabi: Geological Society of America Bulletin, v. 114, p. 259-268.
Wooding, R. A., Tyler S. W., and White, I., 1997, Convection in groundwater below an evaporating salt lake: Onset of instability: Water Resources Research, v. 33, p. 1199-1217.